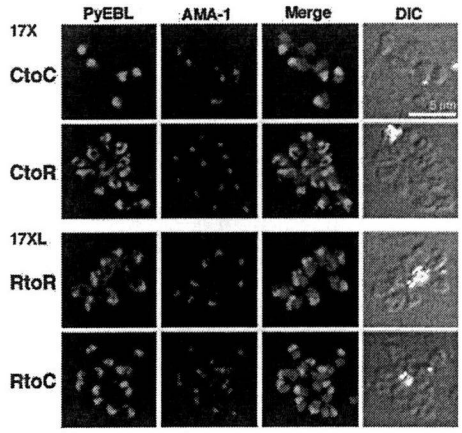

Fig. 4. Replacement of Cys to Arg in region 6 altered subcellular localization of *Py*EBL. Schizonts of transgenic parasite lines were incubated with mAb 5B10 (PyEBL), rabbit anti-AMA1 serum (AMA1), and DAPI (blue) for nuclear staining. DIC images are shown in the right-hand column. In the 17X background, control (CtoC) shows an apical *Py*EBL signal colocalized with AMA1, but replaced (CtoR) shows a 17XL pattern. Inversely, 17XL background control (RtoR) shows a diffused nonapical pattern, but replaced to cysteine (RtoC) shows an apical signal colocalized with AMA1.

nonapical diffused pattern, and *Py*EBL did not colocalize with AMA1. Furthermore, the replacement of Arg with Cys in the 17XL line (17XL-RtoC) altered the *Py*EBL localization from a nonapical diffused pattern to an apical pattern. Control parasites did not display altered *Py*EBL localization (Fig. 4). These results confirm that the observed substitution from Cys to Arg is responsible for the altered localization of *Py*EBL from micronemes to dense granules in the 17XL line.

EBL Localization Alters Erythrocyte-Type Preference and Course of Infection. To determine whether altered localization of *Py*EBL affects erythrocyte-type invasion preference, infected erythrocytes were examined by microscopy, and a selectivity index (SI) was obtained by calculating multiple parasite infection of single erythrocytes for each parasite line on postinfection day 3 in mice (13). We found that 17XL-RtoC predominantly invaded reticulocytes in the same way as the nonlethal 17X line. The SI of the 17XL line (2.38) was increased in 17XL-RtoC (≈35; $P < 0.001$). On the other hand, 17X-CtoR was able to invade a variety of ages of erythrocytes, including mature erythrocytes, comparable to the lethal 17XL line, with the SI of the 17X line (16.78) reduced in 17X-CtoR (≈4; $P < 0.001$; Table 1). These results demonstrate that the localization of *Py*EBL is responsible for the erythrocyte-type preference of the parasite.

Table 1. Selectivity index of WT and transgenic *Plasmodium yoelii* lines

Parasite	*n*	Selectivity index (range)
17X-CtoR 1	5	3.87 (1.86–5.32)
17X-CtoR 2	5	4.25 (2.38–7.97)
17X-CtoC	5	23.53 (16.49–36.00)
17X	5	16.78 (7.60–24.99)
17XL-RtoC 1	5	34.35 (29.18–38.05)
17XL-RtoC 2	5	35.99 (29.97–42.72)
17XL-RtoR	5	1.31 (0.57–2.13)
17XL	5	2.38 (1.58–3.75)

Selectivity indices were calculated from parasitized Giemsa-stained thin blood films collected from each infection.

Because erythrocyte-type preference frequently correlates with virulence in malaria parasites, we further analyzed the transgenic *P. yoelii* parasites for differences in the course of infection and survival of parasite-infected mice. Mice infected with the 17XL-RtoC line developed significantly lower parasitemias compared with the parental 17XL and control 17XL-RtoR lines (Fig. 5*A*), with 100% survival (Fig. 5*C*), whereas all mice infected with 17XL and 17XL-RtoR lines died by day 7 (Fig. 5*C*). The pattern observed for the 17XL-RtoC line was identical to that observed for the nonlethal 17X line. Thus, trafficking of *Py*EBL to the micronemes causes the virulence of the 17XL line to be reduced to the same level as the nonlethal 17X line, suggesting that *Py*EBL is a critical virulence determinant in the 17XL line. The parasitemia of mice infected with 17X-CtoR increased significantly compared with those infected with parental 17X and control 17X-CtoC lines during the acute phase of infection on days 4 to 5 ($P < 0.001$). However, the parasitemia did not reach the level observed for the lethal 17XL line, and it reduced to the same level observed for the 17X and 17X-CtoC lines by day 9 (Fig. 5*B*). No parasites were detectable by microscopy at day 17 (not shown). This suggests that the 17X-CtoR line is able to invade a greater repertoire of erythrocyte types than 17X but is unable to invade as many types as the 17XL line. This reduced capacity to invade multiple erythrocyte types compared with the 17XL line results in a nonlethal infection, in which all mice survive (Fig. 5*C*). Thus, displacement of the EBL from microneme was not sufficient to make this line fully lethal, suggesting the existence of other determinant(s).

Discussion

The results of this study indicate that replacement of Cys to Arg at the second Cys position of *Py*EBL region 6 is the major

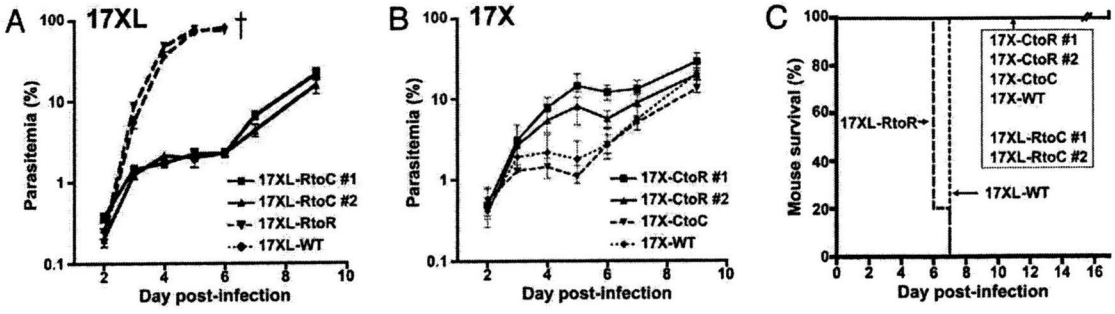

Fig. 5. Effect of the alteration of *pyebl* gene loci on the course of infection and parasite virulence in mice. Mice were i.v. inoculated with 1×10^6 parasitized erythrocytes from WT or transgenic parasite lines. (*A*) Parasitemia of 17XL-RtoC was dramatically reduced to the same level as that of the nonlethal 17X line. (*B*) Parasitemia of 17X-CtoR was significantly higher than parental 17X and control 17X-CtoC on days 4 and 5 ($P < 0.001$), the acute phase of infection; however, the pattern observed is intermediate between the lethal 17XL and nonlethal 17X lines. Parasitemias are plotted using the geometric mean and SD of log-transformed data from groups of 5 mice. (*C*) All mice infected with 17XL-RtoC survived, whereas all mice infected with parental 17XL and control 17XL-RtoR lines died by day 7. All mice infected with 17X, 17X-CtoC, and 17X-CtoR survived.

determinant of the difference between lethal and nonlethal lines of *P. y. yoelii* parasites. This substitution alters the intracellular organelle localization of *Py*EBL from the micronemes to the dense granules and alters the erythrocyte-type invasion preference, course of infection, and parasite virulence in the host.

The crystal structure of region 6 of *P. falciparum* EBA-175 indicates that the second Cys residue forms a disulfide bridge with the fourth Cys residue in this region. Arg substitution of the second Cys residue in the *P. yoelii* 17XL line abolishes this disulfide bridge and thus likely destroys the region 6 structure, which is critical for the trafficking of the protein to the micronemes. It is possible that an incorrectly folded region 6 would not allow the protein to be properly recognized by an (as yet uncharacterized) partner molecule responsible for the trafficking of the EBL protein to the micronemes (9). The mechanism involved in the trafficking of the mutated protein to the dense granules remains unresolved.

Using genetic modification, we have demonstrated that when *Py*EBL is trafficked to the microneme in the 17XL line genetic background, the erythrocyte-type invasion preference and the course of infection are comparable to those of the nonlethal 17X line. This indicates that the substitution of Cys to Arg is a major determinant of the lethal phenotype of the 17XL line. However, when *Py*EBL was not trafficked to the microneme in parasites with the 17X line genetic background, the course of infection was intermediate between the 2 parental lines, suggesting that although *Py*EBL is a critical determinant, other factor(s) are also involved in the lethal phenotype of the 17XL line. In *P. falciparum*, the expression of EBL seems to be co-operationally regulated with another *Plasmodium* ligand encoded by the *rbl (reticulocyte-binding-like)* multigene family that is composed of 6 members in *P. falciparum* and at least 14 members in *P. yoelii* (14–16); thus, the *P. yoelii rbl* protein, Py235, is a potential candidate for such factor(s). Consistent with this hypothesis is the finding that when Py235 expression was suppressed, the course of infection of the lethal *P. yoelii* YM line was altered from a lethal pattern to an intermediate pattern similar to that observed in the 17X-CtoR line shown in this study (17). On the basis of these observations, we propose that *Py*EBL may preferentially recognize reticulocytes and that the removal of *Py*EBL from the micronemes may result in free space within this organelle that may subsequently be filled with other ligand(s), possibly Py235, which consequently enables the parasite to invade a variety of erythrocyte types. Because different Py235 proteins may have different receptor specificities, parasite invasion preference and the subsequent course of infection may vary, depending on the Py235 member that fills the free space in the micronemes created by the absence of *Py*EBL. Such a switching mechanism for an erythrocyte invasion pathway has been previously proposed for *P. falciparum* (18).

A Linkage Group Selection analysis conducted by Pattaradilokrat et al. (19) identified a chromosomal region that included the *ebl* gene locus as a major determinant in the multiplication rate differences between the lethal *P. y. yoelii* YM line and a nonlethal 33X line, supporting the role of the EBL protein in controlling virulence phenotypes. Consistent with our findings that another genetic factor may be involved, they also identified a further genomic region on *P. yoelii* chromosome 5 or 6 that showed weak association with multiplication rate.

Because *Py*EBL localized in the dense granules is potentially nonfunctional, we attempted to disrupt the *pyebl* gene locus in both the 17X and 17XL lines (Fig. S7). However, repeated attempts failed to achieve this, despite the successful genomic integration of the control plasmid. This indicates that *Py*EBL is essential for parasite survival, even when it is not trafficked to the microneme. Two possible explanations for this may be that (*i*) an undetectable amount of *Py*EBL may still localize in the micronemes and remain functional, or (*ii*) *Py*EBL is functional during erythrocyte invasion (or for another unknown critical role during the life cycle), even when localized in the dense granules. Although a subgroup of the dense granules, known as exonemes, were recently reported to secrete their contents immediately before schizont rupture (20), we found that *Py*EBL was not detected on the surface of released individual merozoites of 17XL parasites (Fig. S8). Thus, the identity of the *Py*EBL-containing dense granules and the timing of *Py*EBL secretion from them, if at all, in the 17XL line remain undetermined.

In summary, we have found that a single nucleotide substitution altered the intracellular localization of the malaria parasite ligand *Py*EBL, which in turn altered erythrocyte invasion preference, course of infection, and parasite virulence. The virulence-mediating mechanism described in this report furthers our understanding of parasite–host interactions and has important implications for malaria vaccine design, especially those based on *Pv*DBP for *P. vivax* malaria.

Materials and Methods

Rodent Malaria Parasites. *Plasmodium yoelii* 17X, 17XL, and YM lines were maintained in BALB/c mice (Charles River Japan). The *P. yoelii* YM line was a kind gift from David Walliker of Edinburgh University.

DNA and RNA Isolation. Parasite genomic DNA (gDNA) was isolated from parasite-infected mouse blood using DNAzol BD reagent (Invitrogen). Parasite-infected blood was passed through a single CF11 cellulose column to remove leukocytes, and a schizont-enriched fraction was collected by differential centrifugation on a 50% Percoll solution (GE Healthcare). Total RNA was isolated from the schizont-enriched fraction using RNeasy Mini Kit (Qiagen). cDNA was synthesized using Omniscript reverse transcriptase (Qiagen) with random hexamer after DNase treatment.

PCR Amplification and Sequencing of *ebl* Genes. *ebl* genes were PCR-amplified from gDNA using KOD Plus DNA polymerase (Toyobo), with specific primers for each *ebl* gene designed using the *P. yoelii* genome database (The Institute for Genomic Research) and the *P. chabaudi* and *P. berghei* genome databases (The Sanger Centre). *ebl* sequences were determined by direct sequencing using an ABI PRISM 310 genetic analyzer (Applied Biosystems) from PCR-amplified products. Sequences were aligned using CLUSTALW implemented in MacVector (version 9.0; Accelrys).

Southern Blot Analysis. Five micrograms of *P. yoelii* gDNA were digested with EcoRI, EcoRV, ClaI, BanI, NspI, and with BanI and HpaI with appropriate buffer, overnight. Digested gDNA was subjected to electrophoresis on 0.8% agarose gels, followed by alkaline transfer onto a Hybond-*n* + PVDF membrane (GE Healthcare). Probes were first PCR-amplified with 5′–TAAATCTAAATGGGATACAT–3′ and 5′–AGTTGGATTGATAGTTACAGATTC–3′ primers for the *pyebl* region, cloned into pGEM-T Easy plasmid (Promega), digested from the plasmid, and then hybridized onto membranes. Probes were labeled with the AlkPhos Direct kit (GE Healthcare), and a chemiluminescent signal developed with CDP-*star* reagent (GE Healthcare) was recorded on RX-U film (Fujifilm).

Recombinant Proteins. Expression plasmids were constructed on the basis of the pEU-E01-G(TEV)-N2 vector (21) by inserting PCR products amplified from *P. yoelii* 17X gDNA using KOD Plus DNA polymerase with the following primers: 5′-gagaCTCGAGGTTAATTTATTAAAAAGAACATATGAATCTTTCC-3′ and 5′-tctcGGATCC**CTA**TGAATAGCTCTCTTTTTGAAAAC-3′ for *Py*EBL regions 1 to 6 (R1–6; amino acid positions 28–787), 5′-gagaCTCGAGGTTAATTTATTAAAAAGAACATATGAATCTTTCC-3′ and 5′-tctcGGATCC**CTA**CAAATTATTATTAATAGGAGTATTACTGGG-3′ for regions 1 to 2 (R1–2; 28–436), 5′-gagaCTCGAGGAAAAAAATGGAAATGTAAATTACAAAG-3′ and 5′-tctcGGATCC**CTA**CAAATTATTATTAATAGGAGTATTACTGGG-3′ for region 2 (R2; 113–436), 5′-gagaCTCGAGTCTTCTGTTAAACCCAGTAATAC-3′ and 5′-tctcGGATCC**CTA**TACATTTTCGTTGGCTAGC-3′ for regions 3 to 5 (R3–5; 423–716), and 5′-gagagagaCTCGAGGACCCTAAACATGTATGTGTTGATAC-3′ and 5′-gagagagaGGATCC**TCA**TCCCATAAAGCTGGAAGAACTACAG-3′ for the 19-kDa region of the merozoite surface protein 1, *Py*MSP1 (*Py*MSP1–19; 1658–1757). The stop codon is shown in bold letters, and XhoI and BamHI restriction sites are underlined. GST-fused *Py*EBL or *Py*MSP1–19 recombinant proteins were expressed using the wheat germ cell-free protein synthesis system (Protemist DT; CellFree Sciences). Recombinant proteins were captured by a glutathione

column, washed, and eluted with glutathione elution buffer. Protein synthesis was confirmed by SDS-PAGE and Coomassie Brilliant Blue protein staining. Recombinant *Py*EBL R1–6 and R3–5 and *Py*MSP1–19 were used to produce antibodies, and *Py*EBL R1–2 and R2 were used for Western blot analysis.

Antibodies. To produce mouse anti-*Py*EBL and anti-*Py*MSP1 sera, female BALB/c mice were i.p. immunized 5 times with recombinant *Py*EBL R1–6 or 3 times with recombinant *Py*MSP1–19 emulsified with Freund's adjuvant, and killed for serum collection. To produce rabbit anti-*Py*EBL R3–5 serum, a female Japanese white rabbit was s.c. immunized 3 times with recombinant *Py*EBL R3–5 emulsified with Freund's adjuvant. To produce mouse anti-*Py*EBL monoclonal antibodies, the spleen was removed from a mouse immunized with recombinant *Py*EBL R1–6, and spleen cells were fused with a mouse myeloma cell line derived from a BALB/c mouse by the conventional polyethylene glycol method. Supernatants of cultured hybridoma colonies were tested with recombinant *Py*EBL R1–6 by ELISA and on *P. yoelii* 17X blood smears by indirect immunofluorescent assay. Positive hybridoma colonies were selected and cloned by 2 rounds of limiting dilution. The epitope region of each monoclonal antibody was tested by Western blot with a panel of recombinant *Py*EBL proteins. Anti-AMA1 rabbit serum was a gift from Carole Long of the National Institutes of Health.

Immunofluorescence Microscopy. *P. yoelii*–infected mouse erythrocytes were smeared onto glass slides, air dried, and stored at −80 °C without fixation. Slides were thawed, acetone-fixed, preincubated with PBS containing 5% nonfat milk at 37 °C for 30 min, incubated with mouse anti-*Py*EBL and rabbit anti-AMA1 sera at room temperature for 1 h, and then incubated with FITC-conjugated goat anti-(mouse IgG and IgM) antibody (Biosource International) and Alexa-546–conjugated goat antirabbit IgG antibody (Molecular Probes) at 37 °C for 30 min. Parasite nuclei were stained with DAPI. Differential interference contrast (DIC) and fluorescent images were obtained using a fluorescence microscope (BX50; Olympus) with a CCD digital camera (DC500; Leica) and processed using Adobe Photoshop CS (version 8.0; Adobe Systems).

Immunoelectron Microscopy. *P. yoelii*–infected mouse blood was fixed in 1% paraformaldehyde–0.1% glutaraldehyde in Hepes-buffered saline and embedded in LR white resin (Polysciences). Sections were blocked for 30 min in PBS–milk–Tween 20, incubated overnight at 4 °C in PBS–milk–Tween 20 containing mouse anti-*Py*EBL R1–6 serum, and then incubated for 1 h in PBS–milk–Tween 20 containing goat antimouse IgG conjugated with gold particles (10 nm diameter; Jansen). Sections were stained with 2% uranyl acetate in 50% methanol and examined by electron microscopy (JEM-1230; JEOL).

Genetic Modification of the *pyebl* Gene Locus. Two basic plasmids, pPbDT3U-B12 and pHDEF1-mh-R12, were constructed. A DNA fragment encoding cyan fluorescent protein was PCR-amplified from pECFP-C1 plasmid (Stratagene) using KOD Plus DNA polymerase with primers 5′-agcGCTAGCGTGAG-CAAGGGCGAG-3′ (NheI site is underlined) and 5′-gacGTCGACGGATCCTCTA-GACTTGTACAGCTCGTCC-3′ (SalI and XbaI sites are underlined, and BamHI site is shown in bold) and ligated into the pGEM-T Easy plasmid. The insert was then digested with NheI and SalI, purified, and ligated into pRGDT-B12 (22) using the NheI and SalI sites, yielding pRCDT-B12. pRCDT-B12 was digested with ClaI and XbaI and filled with an oligonucleotide linker comprising cgatCTCGAGCCCGGGt and ctagaCCCGGGCTCGAGat to generate XhoI (underlined) and SmaI (bold) sites to yield pPbDT3U-B12. pHDEF1-mh (23) was digested with SmaI and ApaI to remove the 3′ untranslated region of histidine-rich protein 2, the ApaI cohesive end was blunted, and a Gateway gene conversion cassette C1 (Invitrogen) was inserted. The XhoI site was destroyed by XhoI digestion, filled in using KOD Plus DNA polymerase, and self-ligated to yield pHDEF1-mh-R12.

To modify the *pyebl* gene locus, a DNA fragment encoding *Py*EBL region 6 to the stop codon was PCR-amplified from gDNA of the *P. yoelii* 17XL line with primers 5′-gCCATGGGAACATAGAGACATTAAAAAAAGC-3′ and 5′-gCTCGAGATAAAAATCTACAGGTATATATTC-3′ (NcoI and XhoI sites are underlined) and cloned into pGEM-T Easy plasmids. The insert was ligated into the NcoI and XhoI sites of pPbDT3U-B12 to yield pR6Cyt-B12. DNA fragments encoding *Py*EBL region 3 to the stop codon were PCR-amplified from cDNA of the *P. yoelii* 17X and 17XL lines with primers 5′-atCTTCTGTTA-AACCCAGTAATAC-3′ and 5′-ccAGATCTTTAATAAAAATCTACAGG-TATATATTC-3′ (BglII site is underlined). PCR products were then ligated into the SmaI site of pR6Cyt-B12, yielding pR6Cyt+R3Cyt(X)-B12 and pR6Cyt+R3Cyt(XL)-B12, respectively. pR6Cyt+R3Cyt(X)-B12 and pR6Cyt+R3Cyt(XL)-B12 were subjected to a BP recombination reaction with the donor vector pDONR221 (Invitrogen) to produce the corresponding entry plasmids pENT.R6Cyt+R3Cyt(X) and pENT.R6Cyt+R3Cyt(XL). These entry plasmids were subjected to a LR recombination reaction (Invitrogen), according to the manufacturer's instructions, with pHDEF-1-mh-R12 to yield replacement constructs pYEBL-R6Cyt+R3Cyt(X) and pYEBL-R6Cyt+R3Cyt(XL), respectively.

P. yoelii schizont-enriched fraction was collected by differential centrifugation on 50% HistoDenz in PBS, and 20 μg of XhoI-digested transfection constructs were electroporated to 5×10^7 of enriched schizonts using the Nucleofector device (Amaxa) with human T cell solution under program U-33 (24). Transfected parasites were i.v. injected into 8-week-old BALB/c female mice, which were treated by i.p. injection with 1 mg/kg of pyrimethamine daily. Before inoculation of 17X line parasites, mice were treated with phenylhydrazine to increase the reticulocyte population in the blood. Drug-resistant parasites were cloned by limiting dilution. Integration of the transfection constructs was confirmed by PCR amplification with a unique set of primers for the modified *pyebl* gene locus, followed by sequencing and Southern blot analysis.

Course of Infection. To assess the course of infection of transgenic and WT parasite lines, 1×10^6 parasitized erythrocytes were injected i.v. into 8-week-old female BALB/c mice. Thin blood smears were made daily, stained with Giemsa's solution, and parasitemias were recorded. Mouse survival was evaluated by the Kaplan-Meier method. Parasitemias of each group were compared by 1-way ANOVA and Tukey's posttest, implemented in Prism 4.0 (GraphPad Software).

Selectivity Index. To compare erythrocyte preference between transgenic and WT *P. yoelii* parasite lines, a SI was calculated as follows: Multiple-infected erythrocytes divided by the expected number of multiple-infected erythrocytes, which was calculated from the number of infected erythrocytes and parasitemia (13). When the preferred erythrocyte type is limited, the observed number of multiple-infected erythrocytes increases. More than 200 parasitized erythrocytes were examined on Giemsa-stained thin blood smears collected on postinoculation day 3. The SI of each group was compared by 1-way ANOVA and Tukey's posttest, implemented in Prism 4.0.

For additional information see *SI Materials and Methods*.

ACKNOWLEDGMENTS. We thank D. Walliker for *P. yoelii* 33X, 33XPr3, and YM lines; C. Long for anti-AMA1 rabbit serum; H. A. del Portillo (Barcelona Centre for International Health Research, Barcelona) for pHDEF1-mh; Y. Tanaka, K. Kameda, and K. Oka (Integrated Center for Science, Ehime University) for their expertise; N. Kangwanrangsan (Ehime University, Matsuyama, Japan) for anti-*Py*MSP1–19 serum; and R. Culleton for critical reading. Preliminary sequence data for *P. berghei*, *P. chabaudi*, and *P. vinckei* were obtained from The Institute for Genomic Research. Animal experiments were carried out in compliance with the Guide for Animal Experimentation at Ehime University School of Medicine. This work was supported in part by Grants-in-Aids for Scientific Research 19790308 (to H.O.), 19590428 (to O.K.), 16390126 and 19390120 (to M. Torii), by Scientific Research on Priority Areas 19041053 (to T.T.) from the Ministry of Education, Culture, Sports, Science and Technology of Japan, and by Japan Society for the Promotion of Science–National University of Singapore Joint Research Program 07039011–000161 (to O.K.).

1. Landau I, Gautret P (1998), in *Malaria: Parasite Biology, Pathogenesis, and Protection*, ed Sherman IW (American Society for Microbiology, Washington, DC), pp 401–417.
2. Yoeli M, Hargreaves B, Carter R, Walliker D (1975) Sudden increase in virulence in a strain of *Plasmodium berghei yoelii*. *Ann Trop Med Parasitol* 69:173–178.
3. Playfair JH, De Souza JB, Cottrell BJ (1977) Protection of mice against malaria by a killed vaccine: Differences in effectiveness against *P. yoelii* and *P. berghei*. *Immunology* 33:507–515.
4. Miller LH, Mason SJ, Clyde DF, McGinniss MH (1976) The resistance factor to *Plasmodium vivax* in blacks. The Duffy-blood-group genotype, FyFy. *N Engl J Med* 295:302–304.
5. Wertheimer SP, Barnwell JW (1989) Plasmodium vivax interaction with the human Duffy blood group glycoprotein: Identification of a parasite receptor-like protein. *Exp Parasitol* 69:340–350.
6. Greenwood BM, et al. (2008) Malaria: Progress, perils, and prospects for eradication. *J Clin Invest* 118:1266–1276.
7. Adams JH, et al. (1992) A family of erythrocyte binding proteins of malaria parasites. *Proc Natl Acad Sci USA* 89:7085–7089.
8. Withers-Martinez C, et al. (2008) Malarial EBA-175 region VI crystallographic structure reveals a KIX-like binding interface. *J Mol Biol* 375:773–781.
9. Treeck M, et al. (2006) A conserved region in the EBL proteins is implicated in microneme targeting of the malaria parasite *Plasmodium falciparum*. *J Biol Chem* 281:31995–32003.

10. Sim BK, Toyoshima T, Haynes JD, Aikawa M (1992) Localization of the 175-kilodalton erythrocyte binding antigen in micronemes of *Plasmodium falciparum* merozoites. *Mol Biochem Parasitol* 51:157–159.
11. Adams JH, et al. (1990) The Duffy receptor family of *Plasmodium knowlesi* is located within the micronemes of invasive malaria merozoites. *Cell* 63:141–153.
12. Torii M, Adams JH, Miller LH, Aikawa M (1989) Release of merozoite dense granules during erythrocyte invasion by *Plasmodium knowlesi*. *Infect Immun* 57:3230–3233.
13. Simpson JA, Silamut K, Chotivanich K, Pukrittayakamee S, White NJ (1999) Red cell selectivity in malaria: A study of multiple-infected erythrocytes. *Trans R Soc Trop Med Hyg* 93:165–168.
14. Stubbs J, et al. (2005) Molecular mechanism for switching of *P. falciparum* invasion pathways into human erythrocytes. *Science* 309:1384–1387.
15. Iyer J, Grüner AC, Rénia L, Snounou G, Preiser PR (2007) Invasion of host cells by malaria parasites: A tale of two protein families. *Mol Microbiol* 65:231–249.
16. Carlton JM, et al. (2002) Genome sequence and comparative analysis of the model rodent malaria parasite *Plasmodium yoelii yoelii*. *Nature* 419:512–519.
17. Iyer JK, Amaladoss A, Ganesan S, Preiser PR (2007) Variable expression of the 235 kDa rhoptry protein of *Plasmodium yoelii* mediate host cell adaptation and immune evasion. *Mol Microbiol* 65:333–346.
18. Duraisingh MT, Maier AG, Triglia T, Cowman AF (2003) Erythrocyte-binding antigen 175 mediates invasion in *Plasmodium falciparum* utilizing sialic acid-dependent and -independent pathways. *Proc Natl Acad Sci USA* 100:4796–4801.
19. Pattaradilokrat S, Culleton RL, Cheesman SJ, Carter R (2009) Gene encoding erythrocyte binding ligand linked to blood stage multiplication rate phenotype in *Plasmodium yoelii yoelii*. *Proc Natl Acad Sci USA*, 10.1073/pnas.0811430106.
20. Yeoh S, et al. (2007) Subcellular discharge of a serine protease mediates release of invasive malaria parasites from host erythrocytes. *Cell* 131:1072–1083.
21. Tsuboi T, et al. (2008) Wheat germ cell-free system-based production of malaria proteins for discovery of novel vaccine candidates. *Infect Immun* 76:1702–1708.
22. Ghoneim A, Kaneko O, Tsuboi T, Torii M (2007) The *Plasmodium falciparum* RhopH2 promoter and first 24 amino acids are sufficient to target proteins to the rhoptries. *Parasitol Int* 56:31–43.
23. Fernandez-Becerra C, de Azevedo MF, Yamamoto MM, del Portillo HA (2003) Plasmodium falciparum: New vector with bi-directional promoter activity to stably express transgenes. *Exp Parasitol* 103:88–91.
24. Janse CJ, et al. (2006) High efficiency transfection of *Plasmodium berghei* facilitates novel selection procedures. *Mol Biochem Parasitol* 145:60–70.

Parasitology International 58 (2009) 243–248

Contents lists available at ScienceDirect

Parasitology International

journal homepage: www.elsevier.com/locate/parint

Enzymatic characterization of the *Plasmodium vivax* chitinase, a potential malaria transmission-blocking target

Satoru Takeo [a], Daisuke Hisamori [a], Shusaku Matsuda [a], Joseph Vinetz [b], Jetsumon Sattabongkot [c], Takafumi Tsuboi [a,d,*]

[a] Cell-Free Science and Technology Research Center, Ehime University, 3 Bunkyo-cho, Matsuyama, Ehime 790-8577, Japan
[b] Division of Infectious Diseases, University of California San Diego School of Medicine 9500 Gilman Drive, 0741 Palade Laboratories, La Jolla, CA 92093-0741, USA
[c] Department of Entomology, Armed Forces Research Institute of Medical Sciences, Bangkok 10400, Thailand
[d] Venture Business Laboratory, Ehime University, 3 Bunkyo-cho, Matsuyama, Ehime 790-8577, Japan

ARTICLE INFO

Article history:
Received 18 November 2008
Received in revised form 29 April 2009
Accepted 2 May 2009
Available online 8 May 2009

Keywords:
Chitinase
Transmission-blocking
Plasmodium vivax
Allosamidin

ABSTRACT

The chitinase (EC 3.2.1.14) of the human malaria parasite *Plasmodium falciparum*, PfCHT1, has been validated as a malaria transmission-blocking vaccine (TBV). The present study aimed to delineate functional characteristics of the *P. vivax* chitinase PvCHT1, whose primary structure differs from that of PfCHT1 by having proenzyme and chitin-binding domains. The recombinant protein rPvCHT1 expressed with a wheat germ cell-free system hydrolyzed 4-methylumbelliferone (4MU) derivatives of chitin oligosaccharides (β-1,4-poly-*N*-acetyl glucosamine (GlcNAc)). An anti-rPvCHT1 polyclonal antiserum reacted with *in vitro*-obtained *P. vivax* ookinetes in anterior cytoplasm, showing uneven patchy distribution. Enzymatic activity of rPvCHT1 shared the exclusive endochitinase property with parallelly expressed rPfCHT1 as demonstrated by a marked substrate preference for 4MU-$GlcNAc_3$ compared to shorter GlcNAc substrates. While rPvCHT1 was found to be sensitive to the general family-18 chitinase inhibitor, allosamidin, its pH (maximal in neutral environment) and temperature (max. at ~25 °C) activity profiles and sensitivity to allosamidin ($IC_{50} = 6$ μM) were different from rPfCHT1. The results in this first report of functional rPvCHT1 synthesis indicate that the *P. vivax* chitinase is enzymatically close to long form *Plasmodium* chitinases represented by *P. gallinaceum* PgCHT1.

1. Introduction

To complete transmission between a vertebrate host and an anopheline mosquito, *Plasmodium* male and female gametes merge in the mosquito midgut to form zygotes that elongate into the invasive motile form, the ookinete. The ookinete must traverse the chitin-containing peritrophic matrix (PM) *en route* to invading the midgut epithelium to become a sporozoite-forming oocyst. The ookinete secretes a chitinase [1] that facilitates this process, as has been shown in gene knockout studies [2,3], membrane feeding assays with a chitinase inhibitor allosamidin [4], and with chitinase-specific antibodies [5,6]. Therefore, the chitinase is a potential target for transmission blocking of malaria with chemical or immunological strategies.

Genes encoding chitinases have been identified from several *Plasmodium* species, but functional analysis including studies on enzymatic activity has only been done with the chitinases PfCHT1 of *Plasmodium falciparum* [7] and PgCHT1 of *P. gallinaceum* [8]. *P. gallinaceum* is the only malaria parasite species in which more than one chitinase genes have been identified. Although both PgCHT1 [4,8] and PgCHT2 [5,8–10] are members of the family 18 chitinases, these enzymes differ significantly in their enzymatic properties including pH optima and quantitative sensitivity to allosamidin [8]. The short form PgCHT2 lacks two structure characteristics present in the long form PgCHT1; 1) a "repeat/insert" region to form a proenzyme domain, between N-terminal signal peptide and a catalytic domain, and 2) a putative chitin-binding domain at the C-terminus. The *P. falciparum* PfCHT1 and the chitinase of the chimpanzee malaria parasite *P. reichenowi* PrCHT1 are short forms; the enzymatic characteristics of PfCHT1 has been experimentally demonstrated to be more similar to the orthologous PgCHT2 than to PgCHT1 [7].

Detailed functional analysis including enzymatic characterization of PvCHT1, the chitinase of the other major human malaria parasite *P. vivax* is fundamental to assessing the potential of *Plasmodium* chitinase as a candidate transmission-blocking target. The deduced amino acid sequence from cloned *pvcht1* [11] indicates that this enzyme is orthologous to the long form of *Plasmodium* chitinase represented by PgCHT1. An unrooted phylogenetic tree of the conserved catalytic domain supports the clustering of PvCHT1 and PgCHT1 (TBLASTN amino acid identity values = 81%/positives = 92%) distant from another

* Corresponding author. Cell-Free Science and Technology Research Center, Ehime University, 3 Bunkyo-cho, Matsuyama, Ehime 790-8577, Japan. Tel.: +81 89 927 8277; fax: +81 89 927 9941.
E-mail address: tsuboi@ccr.ehime-u.ac.jp (T. Tsuboi).

1383-5769/$ - see front matter © 2009 Elsevier Ireland Ltd. All rights reserved.
doi:10.1016/j.parint.2009.05.002

clustering of PgCHT2 (I38%/P61%), PfCHT1 (I37%/P62%) and PrCHT1 (I37%/P61%) [10]. No other chitinase appears to be present in the *P. vivax* genome [12]. Indirect immunofluorescence assay (IFA) using antiserum raised against the synthetic peptide corresponding to the catalytic active site of PgCHT1 detected the protein in *P. vivax* ookinetes [11]. Since it is difficult to obtain sufficient native PvCHT1 protein for functional analysis, analysis of recombinant PvCHT1 (rPvCHT1) *in vitro* is necessary. Given the difficulties of expressing rPvCHT1 in *Escherichia coli* (J. Vinetz, unpublished data), we have utilized a cell-free expression system using wheat germ extracts [13,14] which has been demonstrated to be useful for making recombinant *Plasmodium* proteins [15,16] for obtaining functional rPvCHT1. Use of this system included production not only of the common catalytic domain but also of the chitin-binding domain specific to PgCHT1 and PvCHT1 (long form). The system was

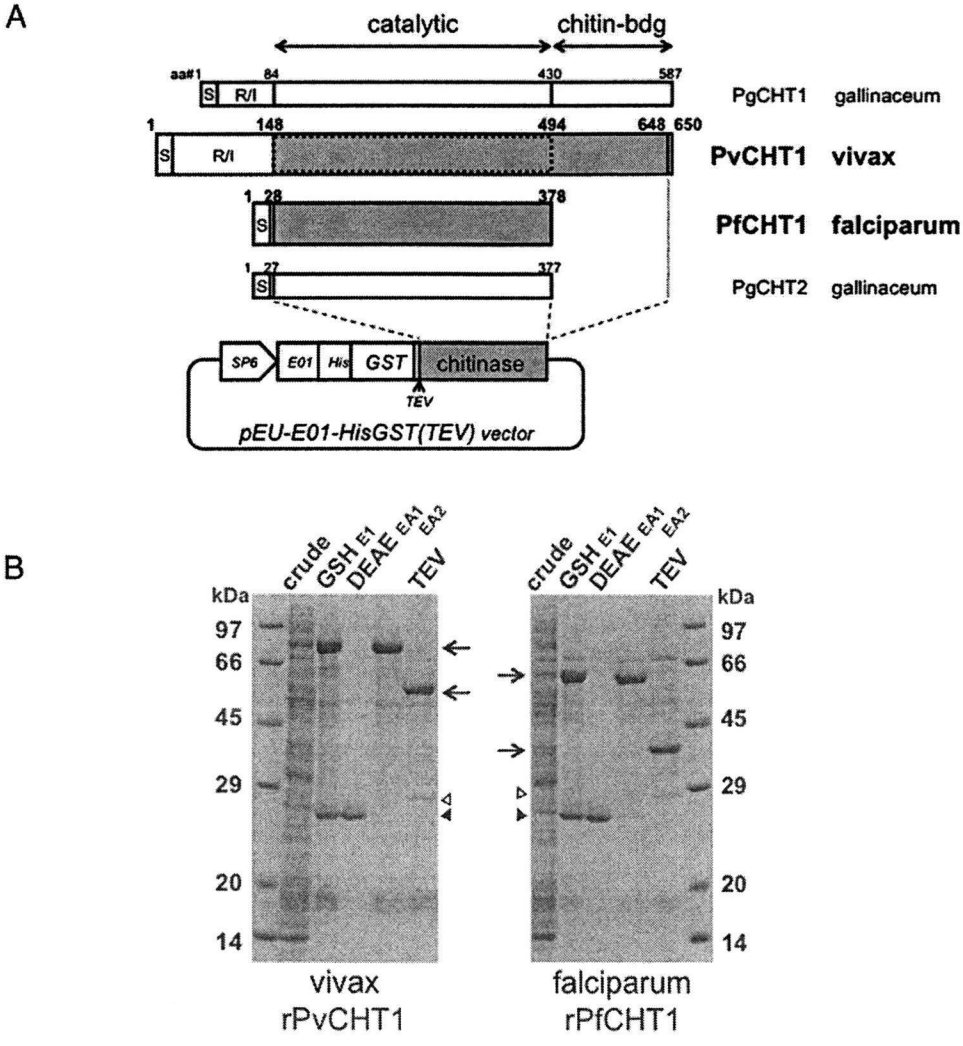

	Protein (μg)		Total activity (*FI / min)		Yield (%)		Specific activity (*FI / min / mg protein)		Fold	
step	vivax	falciparum	vivax	falciparum	vivax	falciparum	vivax	falciparum	vivax	falciparum
GSH E1	636	357	915	153 x 10^3	100	100	1,438	429 x 10^3	1.0	1.0
DEAE EA2	80	29	315	17.8 x 10^3	34	12	3,955	608 x 10^3	2.8	1.4
TEV	33	7	240	14.7 x 10^3	26	10	7,313	2,070 x 10^3	5.1	4.8

*FI : arbitrary relative fluorescence units

Fig. 1. Synthesis and purification of recombinant *P. vivax* chitinase (PvCHT1) and *P. falciparum* PfCHT1 proteins. A. Schematic representation and translated sequence of PvCHT1 and PfCHT1 constructs in a cell-free expression vector pEU-E01-HisGST(TEV). The diagram of two *P. gallinaceum* chitinases PgCHT1 and PgCHT2 as well as the positions of signal peptide (S), repeat/insert region (R/I), and catalytic or chitin-binding domains are placed for comparison. The shaded regions are cloned to obtain recombinant (r) proteins. The second rPvCHT1 mimicking such a short form species as PfCHT1 is bordered by dotted line (see Section 2.1). The locations of SP6 promoter (SP6), translational enhancer (E01), hexa-histidine (His), glutathione S-transferase (GST), and rPvCHT1 or rPfCHT1 (chitinase) on the vector are shown. B. A representative result after sequential purification steps (see Sections 2.3 and 2.4). 2.4 μl of total cell-free synthesis products (crude) or 10 μl of the samples at various purification steps were analyzed by SDS-PAGE under reducing condition. The protein products at each step are shown by arrows. 1) A contaminant glutathione (GSH)-binding protein in the eluates E1 after GSH/GST affinity chromatography, or in EA1 after DEAE anion exchange chromatography, and 2) the remnants of the N-terminal His-GST portion and possibly AcTEV protease itself (28–29 kDa) after AcTEV treatment and dialysis, are respectively shown by closed and open triangles. The chitinase specific activities of rPvCHT1 and rPfCHT1 samples are shown in the table format below; in the eluates E1, EA2, and in the final products after AcTEV treatment and dialysis.

used as well for the *P. falciparum* counterpart PfCHT1 (short form having a catalytic domain only) to allow for direct enzymatic comparison [7].

2. Materials and methods

2.1. Plasmid constructs

The *P. vivax* PvCHT1 expression construct was prepared by PCR-amplifying the native coding sequence from *P. vivax* SalI genomic DNA excluding N-terminal signal peptide and repeat/insert region of *pvcht1* (GenBank accession no. AB106896) (Fig. 1A). The XhoI-containing 5′ primer was GAG ACT CGA GAT GGG AGG TAG CCA TGA TAG AAA ACC TCC (the restriction site underlined, and a start methionine codon typed in italic). The BamHI-containing 3′ primer was GAG AGG ATC CTC ACG CGT CTT CCT CTT GCT CAT AGG G. The deduced PvCHT1 protein begins at Gly-148 immediately downstream from the repeat/insert region, and terminated at Ala-648, the third residue upstream from the C terminus (501 residues). PCR products were restriction-digested, ligated in-frame into the XhoI and BamHI sites of the pEU-E01-HisGST(TEV) expression vector for wheat germ cell-free translation system, a slight modification from original pEU-E01-MCS (CellFree Sciences, Japan. http://www.cfsciences.com/eg/). This vector gives an N-terminal hexa-histidine and glutathione S-transferase (GST) tag followed by a tobacco etch virus (TEV) protease cleavage site upstream of cloned *pvcht1* (Fig. 1A). The construct was transfected into JM109 *E. coli* cells and the correct clone was verified by automated sequencing.

The second PvCHT1 expression construct was established by changing 3′ primer to GAG AGG ATC CTC ACC ATA CAT TCG TAA GGA ACG CAT CTA TAT, which gives shorter PvCHT1 terminating at Trp-494 (347 residues). This shorter construct mimicking such a short form chitinase as PfCHT1 covers only the common domain excluding putative chitin-binding domain (dotted on PvCHT1 in Fig. 1A).

The single copy gene *pfcht1* (accession no. AF172445) of *P. falciparum* chitinase (PfCHT1) was cloned into the same pEU-E01-HisGST(TEV) vector. This clone confers the identical PfCHT1 amino acid sequence, Gly-28 through His-378 (351 residues) to that used for previous study with conventional *E. coli* system [7] (Fig. 1A).

2.2. Recombinant protein synthesis by wheat germ cell-free system

We employed the wheat germ cell-free protein expression system for protein production using the bilayer translation reaction method described previously [13,17]. Briefly, 1.2 ml of transcription mixture containing 120 μg of the pEU vector construct, 80 mM HEPES-KOH, pH 7.8, 16 mM magnesium acetate, 2 mM spermidine, 10 mM dithiothreitol, 2.5 mM each of nucleotide triphosphates, 1 U/μl of SP6 RNA polymerase (Promega), and 1 U/μl of RNasin (Promega) was incubated 6 h at 37 °C. After the incubation, the solution with mRNA was centrifuged at 11,000 ×*g* for 5 min at 4 °C and supernatant was recovered and mixed with an equal volume (1.2 ml) of wheat germ extract (240 A_{260} units) (CellFree Sciences) supplemented with 2.4 μl of 20 mg/ml creatine kinase to prepare translation mixture. On top of 0.4 ml-each mixture aliquot in six-well plate, the 4.4 ml substrate mix containing 30 mM HEPES-KOH, pH 7.8, 100 mM potassium acetate, 2.7 mM magnesium acetate, 0.4 mM spermidine, 2.5 mM dithiothreitol, 0.3 mM each of 20 amino acids, 1.2 mM rATP, 0.25 mM rGTP, and 16 mM creatine phosphate were added and then incubated at 17 °C for 16 h.

2.3. Purification by affinity and anion-exchange chromatography

A 300 μl-bed volume of glutathione-coupled gel (Glutathione Sepharose 4B, GE Healthcare) was pre-equilibrated with 20 mM Tris–HCl (pH 8.0). The whole 28.8 ml of cell-free protein synthesis products was mixed with the gel and incubated for 16 h at 4 °C with gentle agitation. The suspension was then transferred into an empty column (Bio-Spin #732-6008, Bio-Rad Laboratories) and centrifuged at 500 ×*g* for 5 min. After washing the matrix pellet with 20 bed volumes (6 ml) of 20 mM Tris–HCl (pH 8.0), 3 and then 1 bed volume of elution buffer (10 mM reduced glutathione in the Tris-buffer above) were added to collect corresponding eluates E1 and E2.

Anion-exchange column chromatography was conducted on a 150 μl-bed volume of TOYOPEARL DEAE-650-M gel (TOSOH) in Bio-Spin column, pre-equilibrated with 20 mM Tris–HCl (pH 8.0). The E1 eluate above was added to the column and the gel matrix was washed primarily with 1.5 ml of 20 mM Tris–HCl (pH 8.0). The gel was next washed by 0.1 M and then 0.18 M sodium chloride in the same buffer, 0.3 ml each, into the combined eluates EA1. Sodium chloride was concentrated further to 0.5 M (0.75 ml) to collect EA2 eluate.

2.4. AcTEV protease treatment to remove His-GST portion

The 2.5 times EA2 concentrate (0.3 ml) by ultrafiltration (Ultrafree™ #UFV5BGC, 10 kDa molecular mass cutoff, Millipore) was mixed with 10 mU/μl (final) of AcTEV protease (Invitrogen) and incubated for 3 h at 30 °C. 0.2 ml of the product was further mixed with two different matrices, 9 μl of Glutathione Sepharose 4B and 3 μl of nickel-charged resin (Ni-NTA Superflow, Qiagen), pre-equilibrated with 20 mM Tris–HCl (pH 8.0). The mixture was incubated overnight at 4 °C and the supernatant including cleaved PvCHT1 molecules was separated by 0.22 μm microfiltration unit (Ultrafree™ #UFC30GV, Millipore) from His-GST portion on matrices. The solution was dialyzed overnight at 4 °C in the buffer containing 40 mM Tris–HCl, pH 7.5, 400 mM sodium chloride, 2 mM EDTA, and 0.2% TritonX-100. These recombinant PvCHT1 (rPvCHT1) or rPfCHT1 protein samples were finally mixed with an equal volume of 100% glycerol, either for immediate use or for storage at −25 °C until further use.

2.5. Immunization of mice and rabbit with rPvCHT1 and Pvs25

The purified rPvCHT1 proteins were suspended in 1× phosphate buffered saline (PBS). Groups of female BALB/c mice were subcutaneously immunized three times on days 0, 21, and 42 with 10 μg of the rPvCHT1 emulsified in Freund's adjuvant (complete for priming, incomplete Freund's adjuvant for subsequent immunizations). Antiserum was prepared as described elsewhere [18]. For obtaining polyclonal serum for counterstaining, the recombinant ookinete surface protein Pvs25 was administered subcutaneously (250 μg, 3 times) into a Japanese White rabbit following the same protocol [19].

2.6. Indirect immunofluorescence assay (IFA)

Blood specimens from gametocytemic *vivax* malaria patients were used as a source of zygotes/ookinetes produced *in vitro* [20]. The use of all human materials in this study was reviewed and approved by institutional Ethics committee of the Thai Ministry of Public Health and the Human Subjects Research Review Board of the United States Army. Peripheral blood was collected with heparinized syringes with written informed consent from patients who came to the malaria clinics in Mae Sod, Thailand. Infection with *P. vivax* was confirmed by microscopic observation of Giemsa-stained thick and thin blood smears.

Indirect immunofluorescence assays (IFAs) were performed with *P. vivax* zygotes/ookinetes acetone-fixed onto glass slides. After blocking in phosphate-buffered saline (PBS) containing 5% nonfat skim milk, the specimens were incubated 1 h at 37 °C with two primary antibodies in the same buffer, mouse anti-PvCHT1 antiserum (1:50 dilution) and rabbit anti-Pvs25 (1:200). After washing with 1× PBS, slides were then incubated 30 min at 37 °C with Alexa 488-labeled goat anti mouse IgG (1:500 dilution; Invitrogen), Alexa 546-labeled goat anti rabbit IgG (1:500; Invitrogen), and 4,6-diamidino-2-phenyl-indole HCl (DAPI, 1 μg/ml; Wako Pure Chemical). The slides were mounted with Prolong

Gold® (Invitrogen) and examined with LSM5 Pascal confocal laser microscope system (Carl Zeiss MicroImaging).

2.7. Assessment of chitinase activity

Chitinase activity of purified rPvCHT1 or rPfCHT1 aliquots was assayed by microfluorimetry using 4-methylumbelliferone (4MU) derivatives of chitin oligosaccharides (β-1,4-poly-*N*-acetyl glucosamine (GlcNAc)). The reaction volume of 200 µl in 96-well black round bottom plates (Corning) includes 0.1 mM Tris–HCl (pH 8.0), 1 mM sodium chloride, 5 µM EDTA, 0.005% (w/v) Triton X-100, and 19 µM of 4-methylumbelliferyl-*N,N′,N″*-β-D-triacetyl chitotrioside (4MU-$GlcNAc_3$) (Sigma-Aldrich). The production of 4MU during continuous incubation at 26 °C was monitored (Wallac ARVO™ MX 1420 multilabel counter (Perkin Elmer); excitation at 355 nm; emission at 450 nm). The resultant enzymatic activity was reported as initial rates of substrate hydrolysis per minute using a standard curve to transform relative fluorescent units. Quantification of proteins was done using Advanced Protein Assay™ reagent #ADV101 (Cytoskeleton).

2.8. Determination of substrate specificity, pH profile, temperature profile, and allosamidin inhibition curves

To assess substrate specificity of the recombinant *Plasmodium* chitinases, mono-, di-, and tri-GlcNAc derivatives of 4-methylumbelliferone (4MU-$GlcNAc_{1-3}$) (Sigma-Aldrich) were used in enzyme assays under the same conditions as described in Section 2.7. Only 4MU-$GlcNAc_3$ was used for the other three sets of test below. The pH activity profile was monitored at 26 °C using a potassium phosphate buffer (40 mM final with respect to phosphate) system, instead of Tris–HCl, with pH at 4.3 and ranging from 4.5 to 8.0 in 0.5 pH unit increments. The temperature activity profile was tested from 10 to 50 °C in 5 °C increments using standard Tris–HCl (pH 8.0) buffer. An inhibitor against family-18 chitinases, allosamidin (courtesy of Dr. Shohei Sakuda, University of Tokyo, Japan), was prepared as a 4 mM stock in 0.1 M acetate that was diluted just before assay into the standard reaction mixture in the previous section to estimate IC_{50} at fixed 19 µM 4MU-$GlcNAc_3$. The stock allosamidin solution was concentrated so that the solvent acetate did not cause pH fluctuation among working solutions at various allosamidin concentrations (data not shown). These experiments were repeated three times each.

3. Results and discussion

Recombinant protein of a chitinase from *P. vivax* (rPvCHT1) was successfully produced using the wheat germ cell-free translation system (Fig. 1A). rPvCHT1 shared general characteristics with the other *Plasmodium* family-18 chitinases, yet enzymatic characters varied in some details compared to *P. falciparum* recombinant PfCHT1 (rPfCHT1), as described below.

3.1. Enzymatically active PvCHT1 recombinant (r) protein, covering both catalytic and chitin-binding domains, was obtained using the wheat germ cell-free system (Fig. 1B)

A series of rPvCHT1 purification steps produced a prominent protein band with apparent mass of ~80 kDa in the eluate E1 after glutathione (GSH)/glutathione S-transferase (GST) affinity purification, which remained ~80 kDa after anion-exchange chromatography in the eluate EA2, and finally changed to ~60 kDa after AcTEV protease treatment (arrows in Fig. 1B). Another major band with less intensity was at 26–27 kDa in the E1 and separated into EA1 eluate (closed triangle) from the dominant band shown above. This profile is also the case with rPfCHT1; the dominant at 60–65 kDa in the E1 going down to ~40 kDa after AcTEV treatment, while the other band into EA1 at an identical 26–27 kDa indicating a contaminant GSH-binding protein from the wheat germ extract. The profile fits predicted molecular masses: full-length products of 85 kDa (rPvCHT1) or 57 kDa (rPfCHT1) from the constructs in the pEU-E01-HisGST(TEV) should be AcTEV-digested into common 28 kDa N-terminal His-GST portion (open triangle in Fig. 1B) and chitinase part with different sizes (arrows). Using the full long form of rPvCHT1, the chitinase-specific activities digesting 4-methylumbelliferyl-*N,N′,N″*-β-D-triacetyl chitotrioside (4MU-$GlcNAc_3$) were detected compared to mock reactions using protein synthesis products without template mRNA. The rPfCHT1 hydrolyzed 4MU-$GlcNAc_3$ as well, whereas the second (shortened) PvCHT1 construct lacking the putative chitin-binding domain did not show any hydrolyzing activity (data not shown). These results demonstrate for the first time that *P. vivax pvcht1* chitinase can be expressed successfully as an active recombinant protein, and that a putative chitin-binding domain which the *P. falciparum* paralog PfCHT1 lacks at its C-terminus is important for rPvCHT1 to exhibit its enzymatic activity.

Further confirmation of the activity of rPvCHT1 was demonstrated by assays during sequential purification steps. rPvCHT1 chitinase-specific activity increased with purity, but that of rPfCHT1 protein prepared in parallel was >100 times higher than rPvCHT1 at corresponding purification steps. This comparatively weak activity by rPvCHT1 on an artificial substrate 4MU-$GlcNAc_3$ led us to the other test for substrate specificity described in Section 3.3.

3.2. PvCHT1 was localized in cytoplasmic organelle of zygote/ookinete (Fig. 2)

To demonstrate the presence of PvCHT1 in *P. vivax* mosquito midgut stage parasites, immuno-localization assay was carried out. Confocal immunofluorescence microscopy with anti-rPvCHT1 on

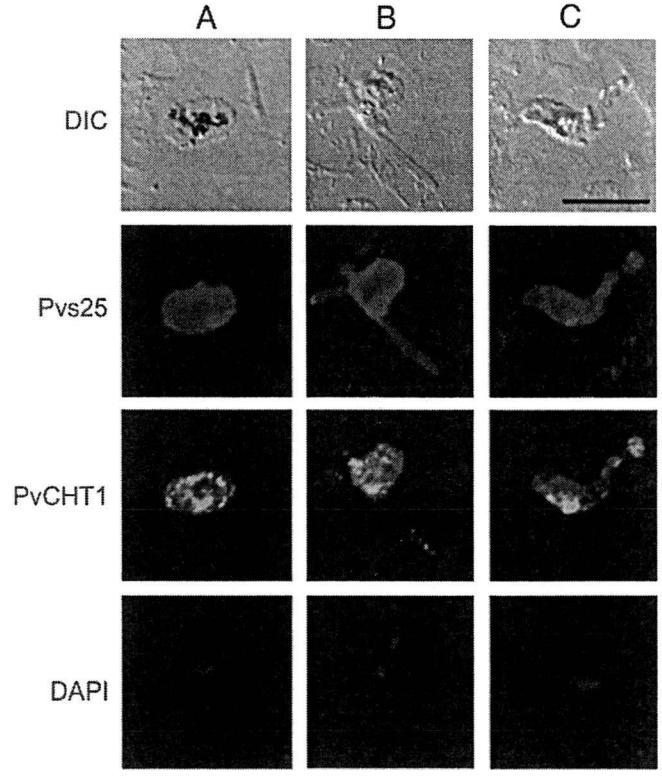

Fig. 2. Immunofluorescence localization of *P. vivax* chitinase PvCHT1 in *in vitro*-developed mosquito midgut stage parasites. Column A (left), zygote; B, immature ookinete; C, mature ookinete. Each of 3 columns consists of 4 panels showing from top to bottom; differential interference contrast (DIC) image, staining with rabbit anti-Pvs25 antiserum (red), with mouse anti-PvCHT1 (green), and DAPI-stained nuclei (blue). Bar = 10 µm. See Section 2.6. (For interpretation of the references to color in this figure legend, the reader is referred to the web version of this article.)

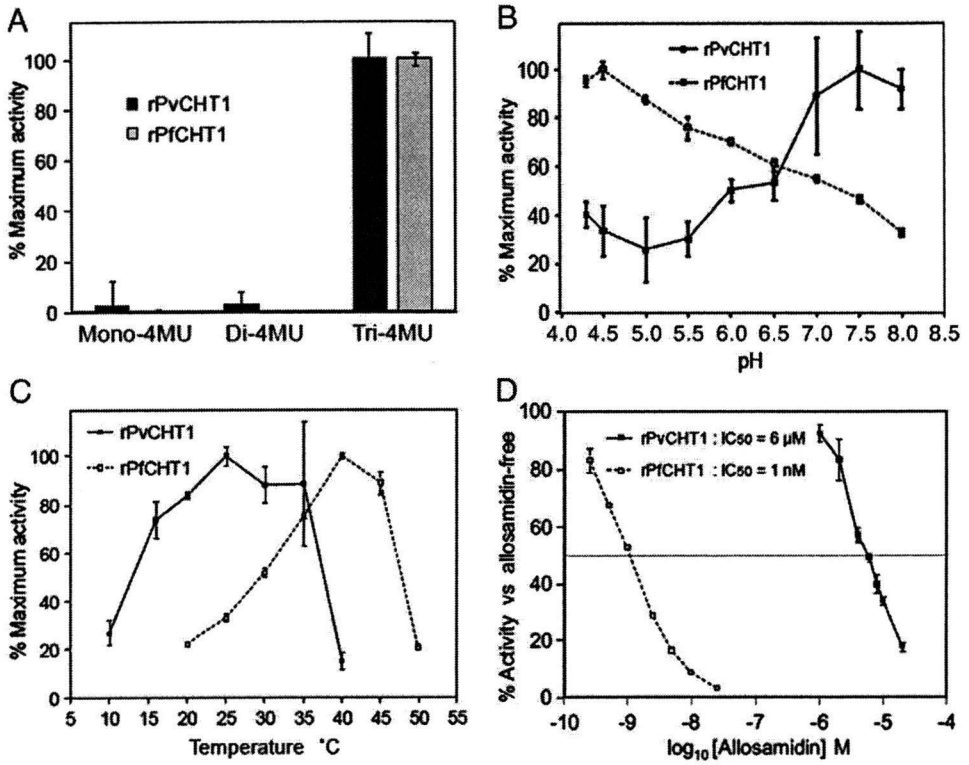

Fig. 3. Detailed analyses of chitinase activities by rPvCHT1 and rPfCHT1. Data with standard errors are displayed as the mean of three separate experiments. See Section 2.8. A. The substrate specificity. Quantification of fluorescence at 26 °C/pH 8.0 on 3 substrates with different number of *N*-acetyl-D-glucosamine (GlcNAc), 4MU-$GlcNAc_{1-3}$. Results are shown as relative rates of activities. B and C. pH or temperature activity profiles. Relative rates of activities at different (B) pH (at a constant temperature of 26 °C) or (C) temperature (at pH 8.0) levels. D. Allosamidin sensitivity on 4MU-$GlcNAc_3$ at 26 °C/pH 8.0. Chitinase activity is expressed as percent activity of enzyme in the absence of allosamidin.

P. vivax zygote/ookinetes demonstrated a nondiffuse, lumpy-granular, and uneven staining (green) throughout the different developmental stages. The PvCHT1 distributed in zygote cytoplasm as granular pattern (Fig. 2, column A), while in immature ookinetes, it was concentrated into zygote remnant space out of which the ookinete is emerging (B). In mature ookinetes there was the patchy appearance of the immunofluorescent signals of PvCHT1 mainly in anterior cytoplasm (C), suggesting the micronemal localization of PvCHT1. This localization was distinct from parasite surface membranes, as delineated by red staining of zygote/ookinete surface antigen Pvs25. The localization pattern of PvCHT1 is consistent with previous IFA studies on *P. gallinaceum* and *P. falciparum* [21] as well as that on *P. vivax* ookinete using anti-*P. gallinaceum* CHT1 active-site antiserum [11], indicating that recombinant PvCHT1 protein with the same immunological properties was successfully prepared.

3.3. The enzymatic characteristics of rPvCHT1, unlike rPfCHT1, were close to plasmodial long form chitinase PgCHT1 (Fig. 3)

We found that rPvCHT1 hydrolyses only 4MU-$GlcNAc_3$ but not 4MU-$GlcNAc_{1-2}$ (Fig. 3A). This substrate preference is shared not only with the rPfCHT1 prepared here with the wheat-germ cell-free system, but is also consistent with previous reports using *E. coli*-produced recombinant PfCHT1 [7] and recombinant PgCHT1 [8]; the same was observed with *P. gallinaceum* native chitinase activity by ookinete crude extracts [8]. These data indicate that PvCHT1 maintains the specificity unique to *Plasmodium* chitinases; an endochitinase with a preference for longer chitin oligosaccharides substrates.

We examined the rPvCHT1 pH activity profile, which demonstrated that optimal activity occurs under neutral condition (pH at 7.0–8.0 in Fig. 3B). It is unique among plasmodial chitinases examined so far, and is consistent with the pH 8.0–9.5 in the adult Anopheles mosquito midgut [22] and further with the pH 7.5–7.6 after bloodmeal ingestion [23]. As a control, rPfCHT1 produced in the wheat germ system was most active at pH 4.5, consistent with previous reports (optimal pH at 4.0–5.0) using native or recombinant proteins PfCHT1, PgCHT1 and PgCHT2 [7,8]. Although the physiological implications in this preference for lower pH by control rPfCHT1 is not instantly clear, it should be noted that the chitinase activity of rPfCHT1 at pH 8.0 still maintains >30% of its maximum at pH 4.5, suggesting that these Pf or Pg chitinases do as well work in the adult mosquitoes midgut. Furthermore, studies on chitinases from microbial sources including bacteria and fungi (Table 1 in review article [24] and references therein) suggest that the difference in optimum pH to this extent is not quite exceptional. The temperature activity profile examined here for the first time even for rPfCHT1 as well as rPvCHT1 (Fig. 3C) showed a preference of rPvCHT1 for relatively lower temperature (maximum at 25 °C and >80% max. at 20–35 °C) than rPfCHT1 (max. at 40 °C). The result is consistent with geographical prevalence of falciparum/vivax malaria; the former is in tropical region and the latter prefers more temperate environment. And it should be noted again that the studies on chitinases from microbial sources (Table 1 in [24]; the optimum Tm ranging from 30 to 60 °C) suggest that the results here by rPvCHT1 and rPfCHT1 are not quite exceptional.

rPvCHT1 was >1,000-fold less sensitive (IC_{50} = 6 µM) to the chitinase inhibitor allosamidin than rPfCHT1 (1 nM), when measured at a fixed concentration of substrate 4MU-$GlcNAc_3$ (19 µM) (Fig. 3D). If *Plasmodium* chitinases are grouped following the *P. gallinaceum* nomenclature into a long form (PgCHT1) and a short form (PgCHT2 lacking a putative chitin-binding domain), this difference was observed previously; the IC_{50} values were 12 µM and 7 µM respectively for recombinant and native PgCHT1 preparation, while as low as 0.3 µM for native PgCHT2 [8]. *P. falciparum* recombinant PfCHT1 produced in *E. coli* showed IC_{50} values around 0.1 µM (40–

150 nM) under different pH conditions of 5.0, 6.0 and 7.0 [7], a sensitivity much closer to its apparent ortholog PgCHT2 than to its paralog PgCHT1. The sensitivity of rPfCHT1 here produced by the wheat germ cell-free system ($IC_{50} = 1$ nM) is even more remarkable, whereas the IC_{50} (6 μM) of rPvCHT1 here is closer to its ortholog PgCHT1. However, it should also be noted that the 1 mM and 0.1 mM concentrations of allosamidin used in previous study to block oocyst development [4] far exceed this value, and they would completely inhibit *P. vivax* chitinase activity *in vivo*.

Collectively, these data in this first report of the functional property of the *P. vivax* chitinase, PvCHT1, indicate that it has most characteristics of *Plasmodium* chitinases. However more in enzymatic detail it is close to long forms represented by *P. gallinaceum* PgCHT1. Also taken into account the difference in the catalytic domain sequence between PvCHT1 and PfCHT1 (Introduction and Fig. 1A), it has yet to be determined whether a single strategy targeting both chitinases is feasible for human malaria transmission-blocking.

Acknowledgements

The authors are grateful for vivax malaria patients at Mae Sod district, Tak Province, Thailand for providing blood specimens, as well as the staff of the Vector Borne Disease Training Center, Pra Budhabat, Saraburi, Thailand, for assistance in setting up the field sites and the staff of the Department of Entomology, AFRIMS, Bangkok, Thailand. A chitinase specific inhibitor allosamidin is a kind gift from Dr. Shohei Sakuda, University of Tokyo, Japan. This work was supported in part by Grants-in-Aid for Scientific Research (17790277, 18390129 and 19406009) and Scientific Research on Priority Areas (19041053) from the Ministry of Education, Culture, Sports, Science and Technology of Japan, and grants from the U.S. National Institutes of Health (JMV).

References

[1] Huber M, Cabib E, Miller LH. Malaria parasite chitinase and penetration of the mosquito peritrophic membrane. Proc Natl Acad Sci U S A 1991;88:2807–10.
[2] Tsai YL, Hayward RE, Langer RC, Fidock DA, Vinetz JM. Disruption of *Plasmodium falciparum* chitinase markedly impairs parasite invasion of mosquito midgut. Infect Immun 2001;69:4048–54.
[3] Dessens JT, Mendoza J, Claudianos C, Vinetz JM, Khater E, Hassard S, et al. Knockout of the rodent malaria parasite chitinase pbCHT1 reduces infectivity to mosquitoes. Infect Immun 2001;69:4041–7.
[4] Shahabuddin M, Toyoshima T, Aikawa M, Kaslow DC. Transmission-blocking activity of a chitinase inhibitor and activation of malarial parasite chitinase by mosquito protease. Proc Natl Acad Sci U S A 1993;90:4266–70.
[5] Langer RC, Li F, Popov V, Kurosky A, Vinetz JM. Monoclonal antibody against the *Plasmodium falciparum* chitinase, PfCHT1, recognizes a malaria transmission-blocking epitope in *Plasmodium gallinaceum* ookinetes unrelated to the chitinase PgCHT1. Infect Immun 2002;70:1581–90.
[6] Li F, Templeton TJ, Popov V, Comer JE, Tsuboi T, Torii M, et al. *Plasmodium* ookinete-secreted proteins secreted through a common micronemal pathway are targets of blocking malaria transmission. J Biol Chem 2004;279:26635–44.
[7] Vinetz JM, Dave SK, Specht CA, Brameld KA, Xu B, Hayward R, et al. The chitinase PfCHT1 from the human malaria parasite *Plasmodium falciparum* lacks proenzyme and chitin-binding domains and displays unique substrate preferences. Proc Natl Acad Sci U S A 1999;96:14061–6.
[8] Vinetz JM, Valenzuela JG, Specht CA, Aravind L, Langer RC, Ribeiro JM, et al. Chitinases of the avian malaria parasite *Plasmodium gallinaceum*, a class of enzymes necessary for parasite invasion of the mosquito midgut. J Biol Chem 2000;275:10331–41.
[9] Langer RC, Li F, Vinetz JM. Identification of novel *Plasmodium gallinaceum* zygote- and ookinete-expressed proteins as targets for blocking malaria transmission. Infect Immun 2002;70:102–6.
[10] Li F, Patra KP, Vinetz JM. An anti-Chitinase malaria transmission-blocking single-chain antibody as an effector molecule for creating a *Plasmodium falciparum*-refractory mosquito. J Infect Dis 2005;192:878–87.
[11] Tsuboi T, Kaneko O, Eitoku C, Suwanabun N, Sattabongkot J, Vinetz JM, et al. Gene structure and ookinete expression of the chitinase genes of *Plasmodium vivax* and *Plasmodium yoelii*. Mol Biochem Parasitol 2003;130:51–4.
[12] Carlton JM, Adams JH, Silva JC, Bidwell SL, Lorenzi H, Caler E, et al. Comparative genomics of the neglected human malaria parasite *Plasmodium vivax*. Nature 2008;455:757–63.
[13] Sawasaki T, Ogasawara T, Morishita R, Endo Y. A cell-free protein synthesis system for high-throughput proteomics. Proc Natl Acad Sci U S A 2002;99:14652–7.
[14] Madin K, Sawasaki T, Ogasawara T, Endo Y. A highly efficient and robust cell-free protein synthesis system prepared from wheat embryos: plants apparently contain a suicide system directed at ribosomes. Proc Natl Acad Sci U S A 2000;97:559–64.
[15] Tsuboi T, Takeo S, Iriko H, Jin L, Tsuchimochi M, Matsuda S, et al. Wheat germ cell-free system-based production of malaria proteins for discovery of novel vaccine candidates. Infect Immun 2008;76:1702–8.
[16] Mudeppa DG, Pang CK, Tsuboi T, Endo Y, Buckner FS, Varani G, et al. Cell-free production of functional *Plasmodium falciparum* dihydrofolate reductase-thymidylate synthase. Mol Biochem Parasitol 2007;151:216–9.
[17] Sawasaki T, Hasegawa Y, Tsuchimochi M, Kamura N, Ogasawara T, Kuroita T, et al. A bilayer cell-free protein synthesis system for high-throughput screening of gene products. FEBS Lett 2002;514:102–5.
[18] Arakawa T, Komesu A, Otsuki H, Sattabongkot J, Udomsangpetch R, Matsumoto Y, et al. Nasal immunization with a malaria transmission-blocking vaccine candidate, Pfs25, induces complete protective immunity in mice against field isolates of *Plasmodium falciparum*. Infect Immun 2005;73:7375–80.
[19] Sattabongkot J, Tsuboi T, Hisaeda H, Tachibana M, Suwanabun N, Rungruang T, et al. Blocking of transmission to mosquitoes by antibody to *Plasmodium vivax* malaria vaccine candidates Pvs25 and Pvs28 despite antigenic polymorphism in field isolates. Am J Trop Med Hyg 2003;69:536–41.
[20] Suwanabun N, Sattabongkot J, Tsuboi T, Torii M, Maneechai N, Rachapaew N, et al. Development of a method for the in vitro production of *Plasmodium vivax* ookinetes. J Parasitol 2001;87:928–30.
[21] Langer RC, Hayward RE, Tsuboi T, Tachibana M, Torii M, Vinetz JM. Micronemal transport of *Plasmodium* ookinete chitinases to the electron-dense area of the apical complex for extracellular secretion. Infect Immun 2000;68:6461–5.
[22] del Pilar Corena M, VanEkeris L, Salazar MI, Bowers D, Fiedler MM, Silverman D, et al. Carbonic anhydrase in the adult mosquito midgut. J Exp Biol 2005;208:3263–73.
[23] Billker O, Miller AJ, Sinden RE. Determination of mosquito bloodmeal pH in situ by ion-selective microelectrode measurement: implications for the regulation of malarial gametogenesis. Parasitology 2000;120(Pt 6):547–51.
[24] Dahiya N, Tewari R, Hoondal GS. Biotechnological aspects of chitinolytic enzymes: a review. Appl Microbiol Biotechnol 2006;71:773–82.

Preerythrocytic, live-attenuated *Plasmodium falciparum* vaccine candidates by design

Kelley M. VanBuskirk[a], Matthew T. O'Neill[b], Patricia De La Vega[c], Alexander G. Maier[b], Urszula Krzych[c], Jack Williams[c], Megan G. Dowler[c], John B. Sacci, Jr.[d], Niwat Kangwanrangsan[e], Takafumi Tsuboi[e], Norman M. Kneteman[f], Donald G. Heppner, Jr.[c], Brant A. Murdock[a], Sebastian A. Mikolajczak[a], Ahmed S. I. Aly[a], Alan F. Cowman[b,1], and Stefan H. I. Kappe[a,g,1]

[a]Seattle Biomedical Research Institute, Seattle, WA 98109; [b]Walter and Eliza Hall Institute, Melbourne, Victoria, Australia 3050; [c]Walter Reed Army Institute for Research, Silver Spring, MD 20910; [d]Department of Microbiology and Immunology, University of Maryland School of Medicine, Baltimore, MD 21201; [e]Department of Molecular Parasitology, Graduate School of Medicine, and Cell-Free Science and Technology Research Center, Ehime University, Matsuyama, Ehime 791-0295, Japan; [f]Department of Surgery, Section of Hepatobiliary, Pancreatic and Transplant Surgery, University of Alberta, Edmonton, Canada T6H 2S2; and [g]Department of Global Health, University of Washington, Seattle, WA 98195

Communicated by Anthony A. James, University of California, Irvine, CA, June 10, 2009 (received for review February 5, 2009)

Falciparum malaria is initiated when *Anopheles* mosquitoes transmit the *Plasmodium* sporozoite stage during a blood meal. Irradiated sporozoites confer sterile protection against subsequent malaria infection in animal models and humans. This level of protection is unmatched by current recombinant malaria vaccines. However, the live-attenuated vaccine approach faces formidable obstacles, including development of accurate, reproducible attenuation techniques. We tested whether *Plasmodium falciparum* could be attenuated at the early liver stage by genetic engineering. The *P. falciparum* genetically attenuated parasites (GAPs) harbor individual deletions or simultaneous deletions of the sporozoite-expressed genes *P52* and *P36*. Gene deletions were done by double-cross-over recombination to avoid genetic reversion of the knockout parasites. The gene deletions did not affect parasite replication throughout the erythrocytic cycle, gametocyte production, mosquito infections, and sporozoite production rates. However, the deletions caused parasite developmental arrest during hepatocyte infection. The double-gene deletion line exhibited a more severe intrahepatocytic growth defect compared with the single-gene deletion lines, and it did not persist. This defect was assessed in an in vitro liver-stage growth assay and in a chimeric mouse model harboring human hepatocytes. The strong phenotype of the double knockout GAP justifies its human testing as a whole-organism vaccine candidate using the established sporozoite challenge model. GAPs might provide a safe and reproducible platform to develop an efficacious whole-cell malaria vaccine that prevents infection at the preerythrocytic stage.

genetically attenuated parasites | malaria vaccine | P36 | P52 | sporozoite

Malaria is a formidable global health problem, affecting 300 million to 500 million people worldwide annually (1). The resulting ≈1 million deaths per year are mainly caused by *Plasmodium falciparum* infections. Eradication of malaria will in large part depend on an effective vaccine that prevents infection by *Plasmodium*, but such a vaccine has remained elusive. The parasites' preerythrocytic stages, encompassing the mosquito-inoculated sporozoites and liver stages that develop from sporozoites after their invasion of hepatocytes, are attractive targets for antiinfection vaccines, because at this stage the number of infected host cells is low, and further transmission of the parasite is not yet possible. Occurrence of blood-stage infection after sporozoite challenge is completely preventable by immunization with radiation-attenuated sporozoites in mouse models of malaria (2). This was a landmark finding that set the standards for malaria preerythrocytic vaccine development. Radiation-attenuated sporozoites arrest in development during hepatocyte infection, but their safety and efficacy are dependent on a precise irradiation dose. Humans immunized with *P. falciparum* radiation-attenuated sporozoites have been effectively protected from subsequent challenge with homologous and heterologous wild type (WT) *P. falciparum* sporozoites (3–5). Therefore, the development of a widely deployable *P. falciparum* radiation-attenuated sporozoite vaccine has been proposed (6). Although genetic manipulation systems are available for *P. falciparum*, they have not been used to develop attenuated parasite strains. Recently, preerythrocytic stages of the rodent malaria parasites *Plasmodium berghei* and *Plasmodium yoelii* were attenuated by deletion of preerythrocytic-stage-expressed genes named Up-regulated in Infectious Sporozoites (UISs). UIS3 and UIS4 (7–9) are proteins of the liver-stage parasitophorous vacuole membrane, the principal host–parasite interface during liver infection (7, 10). Deletion of *UIS3* and *UIS4* led to complete arrest of early liver-stage development after hepatocyte infection (7–9). Deletion of another *UIS* gene, *P52*, encoding a putative GPI-anchored protein (11, 12), and *P36*, a gene encoding a putative secreted protein (12), also resulted in developmental arrest at the early stage of hepatocyte infection. Immunization of mice with *uis3*$^-$, *uis4*$^-$, or *p52*$^-$ parasites induced complete, long-lasting protection against infectious sporozoite challenge (7–9, 11), demonstrating that rodent malaria GAPs are highly effective vaccines. The GAP-induced protection was mediated mainly by CD8$^+$ T cells (9, 13, 14), but antibodies also contributed to protection (9).

To assess the potential to create a GAP vaccine for human malaria, we deleted the *P52* and *P36* loci in *P. falciparum*. The deletions did not affect the parasites throughout most of the life cycle, including sporozoite production of the attenuated lines, but resulted in significant growth defects in a hepatocytic cell line. Furthermore, we report the successful genetic attenuation of *P. falciparum* preerythrocytic stages by simultaneous deletion of *P52* and *P36*, creating a *p52*$^-$/*p36*$^-$ double-gene knockout strain. Dual gene deletions might alleviate safety concerns for the use of GAPs as a vaccine in humans.

Results

***P. falciparum* P52 and P36.** The *P. falciparum* genes *PfP52* (GenBank, XP_001351357; PlasmoDB, PFD0215c) and *PfP36* (GenBank, XP_001351356; PlasmoDB, PFD0210c) are paralogous, tandem-

Author contributions: M.T.O., A.G.M., U.K., J.W., J.B.S., T.T., D.G.H., B.A.M., S.A.M., A.F.C., and S.H.I.K. designed research; K.M.V., M.T.O., P.D.L.V., A.G.M., J.W., M.G.D., J.B.S., N.K., and A.S.I.A. performed research; N.M.K. contributed new reagents/analytic tools; K.M.V., M.T.O., P.D.L.V., U.K., J.W., J.B.S., T.T., B.A.M., S.A.M., A.F.C., and S.H.I.K. analyzed data; and K.M.V., S.A.M., A.F.C., and S.H.I.K. wrote the paper.

Conflict of interest statement: S.H.I.K. is an inventor listed on U.S. Patent No. 7,22,179, U.S. Patent No. 7,261,884, and international patent application PCT/US2004/043023, each titled "Live Genetically Attenuated Malaria Vaccine."

Freely available online through the PNAS open access option.

[1]To whom correspondence may be addressed. E-mail: cowman@wehi.edu.au or stefan.kappe@sbri.org.

This article contains supporting information online at www.pnas.org/cgi/content/full/0906387106/DCSupplemental.

www.pnas.org/cgi/doi/10.1073/pnas.0906387106

arranged genes on chromosome 4. Their products exhibit a predicted N-terminal cleavable signal peptide followed by two 6-Cys domains. In addition, P52 exhibits a C-terminal hydrophobic sequence predicted to be a putative GPI anchor attachment signal (15). *Pf*P52 and *Pf*P36 show 40% and 43% amino acid identity to their respective *P. yoelii* orthologs. To determine the subcellular localization of *Pf*P52 and *Pf*P36, we expressed each protein in a wheat germ cell-free expression system (16). Polyclonal antisera were raised in mice and rabbits, and reactivity was tested in immunofluorescence assays (IFAs) using *P. falciparum* sporozoites. A specific sporozoite-internal staining was observed for P52 that partially colocalized with the micronemal protein TRAP (Fig. S1). The fluorescence was only observed in sporozoites after permeabilization of membranes, indicating that P52 may localize to the secretory organelles of sporozoites. Preimmune sera did not show reactivity with sporozoites. Unfortunately, antisera raised against P36 did not react with sporozoites in IFAs, and therefore protein expression was not determined. However, a recent proteomic study of *P. falciparum* sporozoites detected P36 as well as P52 with multiple peptide hits, showing that both proteins are expressed in this life cycle stage (17).

Deletion of *P. falciparum* P52 and P36. To delete *PfP52* and *PfP36* from the parasite genome, we used a positive–negative selection strategy (18). Double-cross-over homologous recombination between targeting sequences in transfection constructs and the endogenous genes resulted in replacement of *PfP52* and *PfP36* individually with the human dihydrofolate reductase (*dhfr*) selectable marker (19). Two independently transfected lines of the *P. falciparum* gametocyte-producing clone 3D7 were generated for each targeted locus. Transfectant parasites appeared between days 21 and 35 after transfection under positive selection with WR92210 (19). Parental transfectants were removed from positive selection for a 3-week period and then subjected to positive selection until a stable population was established after 2 weeks. This was followed by negative selection against cytosine deaminase-uracil phosphoribosyltransferase with 5-fluorocytosine. Transfectant lines were then analyzed by Southern blotting to detect the gene deletions. Clonal lines of recombinant parasites were derived from the parental population by limiting dilution and were analyzed for successful gene deletion and absence of WT by Southern blotting. The Southern blot analysis confirmed the genetic homogeneity of the knockouts (Fig. S2).

***P52-* and *P36*-Deficient *P. falciparum* Parasites Show Normal Infectivity and Development in the Mosquito.** Deletion of *PfP52* and *PfP36* in the erythrocytic stage did not result in any observable defect during blood-stage replication, indicating that these genes have no apparent critical function during this part of the parasite life cycle. Gametocyte cultures were used to infect *Anopheles stephensi* mosquitoes by membrane feeding. Evaluation of midgut oocyst infection in mosquitoes showed no discernible differences between WT, $p52^-$, and $p36^-$ knockout lines. This indicated that gene deletions did not affect the sexual stages of the parasite. Furthermore, it provided evidence that prolonged culture of knockout parasite lines during drug selection did not significantly reduce knockout parasite transmissibility to mosquitoes. Importantly, invasion of the mosquito salivary glands appeared normal in the *P52* and *P36* knockout lines, because numbers of sporozoites isolated from the glands were comparable to WT sporozoite numbers (Table 1); no significant differences from WT were observed for $p36^-$ ($P = 0.29$) and $p52^-$ ($P = 0.46$).

***P52-* and *P36*-Deficient *P. falciparum* Sporozoites Are Biologically Active.** To ensure that gene deletions resulted in lack of expression of *P52* or *P36*, we performed RT-PCR on sporozoite RNA isolated from WT and knockout parasite lines (Fig. S3*A*). Results indicated that $p52^-$ sporozoites did not express intact transcripts for *P52* but expressed transcripts for *P36*; conversely, $p36^-$ knockout sporozoites expressed transcripts for *P52* but not for *P36*. It has been shown that the biological activity of sporozoites is reflected in their motility on a solid substrate that can be assessed by detecting shed circumsporozoite (CS) protein, the main sporozoite surface protein (20). No significant differences in motility and CS protein shedding were observed between WT and $p52^-$ ($P = 0.59$) or $p36^-$ ($P = 0.29$) lines, as evidenced by quantification of trails stained with anti-CS protein antibodies (Fig. S3 *B–D*, Table 1, and Table S1).

Table 1. Phenotypic analysis of *Pf p52*$^-$ and *Pf p36*$^-$-deficient sporozoites and liver stages

Parasite line	Salivary gland sporozoites per mosquito	Motility assay*	Invasion assay†	Liver-stage parasite abundance‡
Pf WT	45,233 ± 24,624	1.00	1.00	1.00
Pf p52$^-$	57,162 ± 7,535	0.92 ± 0.11	1.04 ± 0.07	0.70 ± 0.11
Pf p36$^-$	67,667 ± 29,365	0.92 ± 0.13	1.00 ± 0.13	0.65 ± 0.10

*Determined by counting CS protein sporozoite trails.
†Sporozoite invasion of HC-04 cells.
‡Determined at 72 h after infection.

***P52-* and *P36*-Deficient *P. falciparum* Parasites Invade Host Cells but Exhibit Developmental Arrest in a Hepatocytic Cell Line.** We investigated the ability of $p52^-$ and $p36^-$ sporozoites to invade host cells in vitro by using the HC-04 cell line, which supports invasion and complete liver-stage development of *P. falciparum* (21). Invasion was assessed microscopically by counting the number of cells invaded by sporozoites. Invasion rates were comparable among WT and knockout parasite lines, indicating that the lack of P52 or P36 did not impact sporozoite host cell entry (Table 1 and Table S2), because no significant differences between hepatocyte invasion rates of WT and the $p52^-$ ($P = 0.29$) or $p36^-$ ($P = 0.59$) were observed.

Next, intracellular development of the knockout parasite liver stages was compared to WT parasite development in HC-04 cells at 3, 4, and 6 days after sporozoite infection (Fig. 1, Table 1, and Table S3). Overall numbers of intrahepatocytic parasites observed

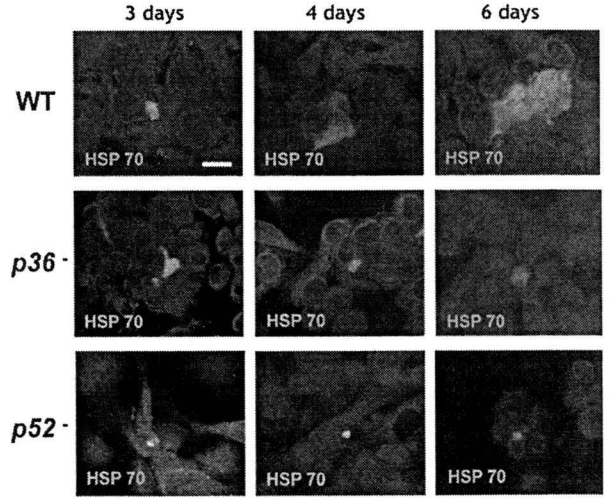

Fig. 1. The *p52*- and *p36*-deficient *P. falciparum* parasites show defective liver-stage development. Development of mutant and WT liver stages was assessed in vitro by using cultured cells of the HC-04 human hepatocytic line. Parasite growth was monitored over 6 days, and liver stages were visualized by immunofluorescence microscopy at 400× magnification with anti-HSP70 at 3, 4, and 6 days after infection. *P. falciparum* $p52^-$ and $p36^-$ parasites exhibited abnormal, arrested development that is most apparent at the 6-day developmental time point. (Scale bar: 10 μm.)

MICROBIOLOGY

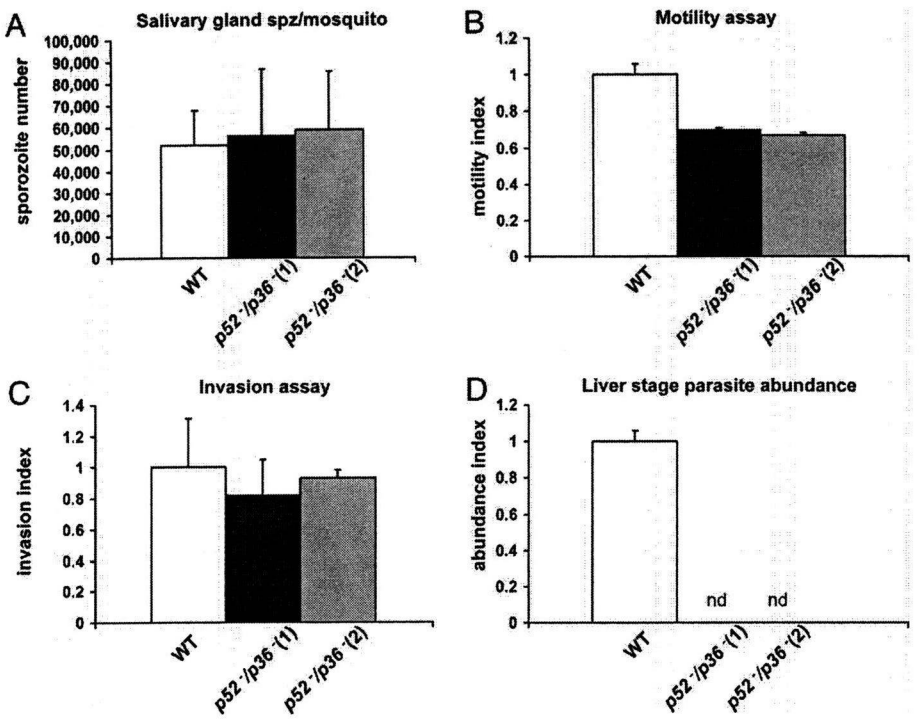

Fig. 2. Phenotypic analysis of *P. falciparum* *p52⁻/p36⁻*-deficient sporozoites and liver stages reveals a severe defect in liver-stage development. (*A*) The *p52⁻/p36⁻* parasites show normal invasion of the mosquito salivary glands; no significant differences were observed between WT and the double-knockout clones ($P = 0.89$). (*B*) The *p52⁻/p36⁻* parasites showed slightly lower gliding activity compared with WT parasites; the effect was not statistically significant at the 95% confidence level ($P = 0.11$). (*C*) WT and *p52⁻/p36⁻* parasites have comparable ability to enter hepatocytes; no significant difference was seen between *p52⁻/p36⁻* and WT parasites ($P = 0.11$). (*D*) The double-knockout parasites show a severe developmental arrest and do not persist, because no *p52⁻/p36⁻* liver stages are detected at 4 days after HC-04 cell line invasion. Statistical differences between the mutant and WT parasite lines were evaluated by the Wilcoxon matched-pairs, signed-rank test. nd, not detected.

in vitro at 72 h after invasion appeared lower in knockout parasites when compared to WT (Table 1), but the difference was not significant for *p52⁻* ($P > 0.99$) or *p36⁻* ($P = 0.11$). However, at day 4, knockout parasite liver stages exhibited smaller sizes in infected HC-04 cultures when compared to WT parasites, and at day 6 knockout parasite liver stages showed severe growth arrest when compared to well-developed WT parasite liver stages (Fig. 1).

Production and Evaluation of *P. falciparum* *p52⁻/p36⁻* Double-Deficient Parasite Lines. We next simultaneously deleted *P52* and *P36* from the parasite genome. Because *PfP52* and *PfP36* are tandem-arranged in the parasite genome, we deleted both genes in a single double-cross-over homologous recombination event (Fig. S4). Similarly to single deletion of *P52* or *P36* knockout lines, the double-deletion knockout lines showed no observable defects in blood-stage replication, the morphology of gametocytes, male gamete exflagellation, and oocyst development in the mosquito midgut. RT-PCR performed on *p52⁻/p36⁻* sporozoites confirmed a lack of intact transcripts for both genes (Fig. S5*A*). We were also able to isolate *p52⁻/p36⁻* mosquito salivary gland sporozoites in numbers comparable to WT salivary gland sporozoites ($P = 0.89$) (Fig. 2*A*). Similarly to individual deletions of *P52* or *P36*, the simultaneous deletion of *P52* and *P36* did not result in a major decrease of sporozoite biological activity, as determined by evaluation of gliding motility [*p52⁻/p36⁻* showed slightly lower gliding motility activity compared with WT parasites, but the effect was not statistically significant at the 95% confidence level ($P = 0.11$)]. Neither did the *p52⁻/p36⁻* parasite lines show a difference in their ability to enter hepatocytes compared with WT ($P = 0.11$) (Fig. 2 *B* and *C*, Fig. S5 *B* and *C* and Tables S4 and S5). Importantly, however, the *p52⁻/p36⁻* parasites showed a more severe developmental arrest in hepatocytes when compared to the *P52*- or *P36*-deficient parasites. Intrahepatocytic *p52⁻/p36⁻* parasites were only rarely detectable 3 days after HC-04 infection (Fig. S5*D*) and were not detectable 4–6 days after infection of the HC-04 cell line (Fig. 2*D*, Table 2, and Table S6). We further evaluated the degree of attenuation of *p36⁻*, *p52⁻* single-knockout and p52⁻/*p36⁻* double-knockout liver stages at 72 h (Table 3) and at 144 h after infection in the HC-04 cell line (Table 2) by using antibodies to known liver-stage-expressed antigens. At 72 h after infection, the expression profile of *p36⁻* and *p52⁻* single knockouts and p52⁻/*p36⁻* double knockout resembled the staining profile of WT liver stages, including expression of LSA-1 (Table 3). At 144 h after infection, *p36⁻* and *p52⁻* continued to show expression of LSA-1, but we could not detect expression of EBA175 (a late liver-stage/blood-stage marker) (22). Staining of p52⁻/*p36⁻* liver stages at 144 h after infection could not be evaluated because no parasites were detectable at this time point with any of the tested antibodies (Table 2). Our data show that individual gene deletions of P36 and P52 result in a liver-stage growth defect. The *p36⁻* and *p52⁻* lines express liver-stage antigen but fail to continue development and do not initiate expression of blood-stage antigen. However, they survive inside HC-04 cells, at least until day 6 after infection. In contrast, the *p52⁻/p36⁻* double knockout not only shows a severe growth defect but also cannot survive beyond day 3 after infection.

***P. falciparum* *p52⁻/p36⁻* Double-Deficient Sporozoites Fail to Productively Infect the Livers of Humanized SCID Alb-uPA Mice.** The liver phase of *P. falciparum* develops only in human hepatocytes, and it

Table 2. Staining profile of liver stages at 144 h after infection

Marker	*Pf p36⁻*	*Pf p52⁻*	*Pf p52⁻/p36⁻*	WT
CSP	Positive (faint)	Positive (faint)	ND	Positive (faint)
HSP70	Positive	Positive	ND	Positive
LSA 1	Positive	Positive	ND	Positive
EBA175	Negative	Negative	ND	Positive

ND indicates liver stages not detected.

Table 3. Staining profile of liver stages at 72 h after infection

Marker	*Pf p36⁻*	*Pf p52⁻*	*Pf p52⁻/p36⁻*	WT
CSP	Positive	Positive	Positive	Positive
HSP70	Positive	Positive	Positive	Positive
LSA 1	Positive	Positive	Positive	Positive
EBA175	Negative	Negative	Negative	Negative

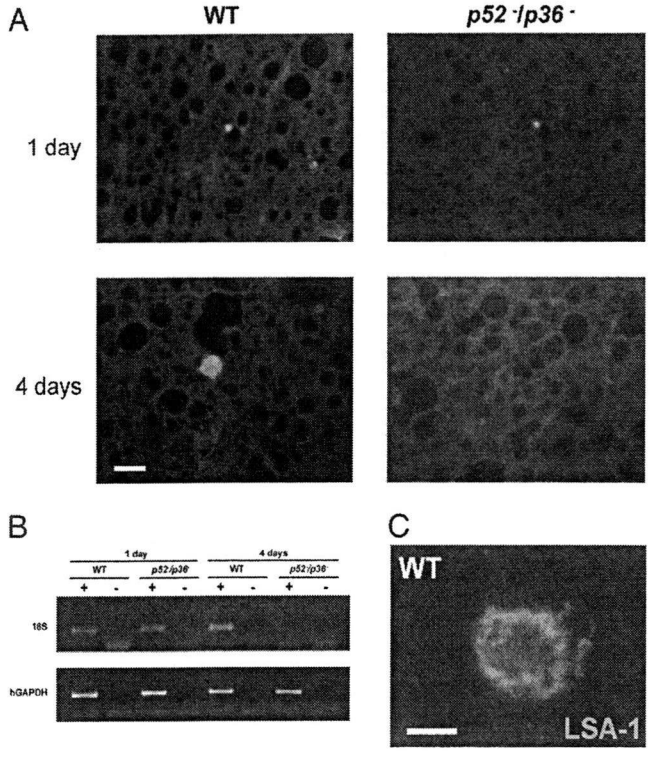

Fig. 3. *P. falciparum p52⁻/p36⁻* parasites do not grow and persist in a humanized chimeric liver mouse model. SCID Alb-uPA mice were inoculated with 10^6 primary human hepatocytes to create chimeric human–mouse livers. Mice positive for engraftment were infected intravenously with 1×10^6 sporozoites of either *p52⁻/p36⁻* or WT *P. falciparum*. (*A*) Immunofluorescent micrographs of chimeric SCID/*Alb-uPA* liver cryosections after WT *P. falciparum* infection, stained with parasite-specific antibodies. Tissue was harvested at 1 day or 4 days after mice were inoculated with *P. falciparum* sporozoites. Sections in panels were stained with an anti-*Pf*HSP70 monoclonal antibody. The data show that *p52⁻/p36⁻* liver stages are detected 1 day after infection but are not detected 4 days after infection. (Scale bar: 10 μm.) (*B*) RT-PCR analysis was performed with RNA isolated from individual livers of chimeric mice 1 day or 4 days after infection. Total RNA was extracted, and reverse-transcription reactions were done with (+) or without (−) the reverse transcriptase. Primers specific for the 18S (small-subunit) ribosomal RNA of *P. falciparum* and human glyceraldehyde phosphate dehydrogenase (hGAPDH) were then used to amplify the reverse-transcribed message. The GAPDH control reaction was positive for samples from all of the mice. The parasite-specific 18S reaction was positive for the mice infected with the WT parasites at day 1 and day 4 after infection. For the double-knockout parasite-infected mice, the 18S reaction was only positive for tissues harvested 1 day after infection and negative for tissue harvested at 4 days after infection, indicating that *p52⁻/p36⁻* parasites were no longer present in the liver at the later time point. RT-PCR was performed on all mice used in the experiment, and results were consistent with the results shown here. (*C*) An example of WT *P. falciparum* liver stage from chimeric SCID/*Alb-uPA* liver cryosection stained with polyclonal rabbit antisera against the repeat region of LSA-1 at 4 days after infection. (Scale bar: 5 μm.)

is not adequately assessed in conventional animal models. Therefore, we used a humanized mouse model (23) to study infectivity of the double-knockout parasite *p52⁻/p36⁻*. Immunodeficient mice homozygous for the urokinase-type plasminogen activator transgene (SCID Alb-uPA) were inoculated with 10^6 primary human hepatocytes to create chimeric human–mouse livers (24). After 6 weeks, successful engraftment was evaluated (Table S7). Positive engrafted chimeric mice were infected intravenously with 10^6 sporozoites of either *p52⁻/p36⁻* ($n = 3$) or WT ($n = 3$) *P. falciparum*, and livers were harvested 1 day or 4 days after infection. Tissue sections of livers were labeled with antisera against parasite HSP70 (Fig. 3*A*), LSA-1 (Fig. 3*C*), and CS protein and were examined by immunofluorescence microscopy. The *p52⁻/p36⁻* and WT liver stages were easily detected at 1 day after infection by microscopy and by amplification of parasite 18S rDNA (Fig. 3*A* and *B*). Enumeration of intrahepatic parasites using microscopic counting showed no significant difference between WT (22 ± 5.5 per square centimeter of tissue) and *p52⁻/p36⁻* knockout (20 ± 3.2 per square centimeter of tissue) 1 day after infection. However, no *p52⁻/p36⁻* parasites were detected at 4 days after infection by using microscopy and RT-PCR, whereas WT parasites were easily detected in both assays (Fig. 3 *A* and *B*).

Together, the data obtained with HC-04 assays and chimeric mouse infections indicate that the *P. falciparum p52⁻/p36⁻* double-knockout GAP infects human hepatocytes but is more severely attenuated then the single-knockout GAPs, cannot successfully develop in human hepatocytes, and does not persist beyond day 4 of infection.

Discussion

Malaria remains a major public health threat in the developing world, with most deaths attributed to *P. falciparum* infection (1, 25). Radiation-attenuated, sporozoite-mediated sterile protection has served as a paradigm to guide the search for a recombinant preerythrocytic vaccine candidate but was not considered a viable solution to malaria vaccine development until recently (6). Yet, a vaccine against the parasite is not available, and the most advanced recombinant vaccine, RTS/S, which is based on the CS protein, conferred significant but limited protection against infection (26, 27). A significant breakthrough toward feasibility of a live-attenuated malaria vaccine was the demonstration of genetic attenuation by gene deletions in rodent malaria models. GAP vaccinations confer sterile, long-lasting protection against high-dose WT sporozoite challenge in mice (7–9, 11). However, it has remained unknown whether precise genetic attenuation, and thus the development of an engineered live-attenuated candidate vaccine strain of *P. falciparum*, is feasible.

Here, we targeted two sporozoite-expressed loci in *P. falciparum*—*P52* and *P36*—for deletion. Deletion of the orthologous genes in the rodent malaria models had indicated that they are important for productive liver infection (11, 12, 28). Transmission to the mosquito vector and passage through the mosquito stages were not affected by deletion of either *P52* or *P36*. Furthermore, although loss of gametocyte production and transmissibility has been reported after prolonged culture of *P. falciparum* (29, 30), the selection procedure for cytoadherence we used to minimize loss of chromosome ends (31) appeared to have circumvented this problem.

Analysis of the *p52⁻* and *p36⁻* lines showed normal mosquito salivary gland infection rates, and knockout salivary gland sporozoites exhibited normal gliding motility, demonstrating that the viability of knockout sporozoites was not affected up to this point in the parasites' developmental progression. Further analysis of the human parasite preerythrocytic stages has been challenging because no practical animal models for in vivo evaluation of liver infection exist. Nonetheless, liver infection can be modeled in cell culture, and we made use of the HC-04 continuous hepatocytic cell line that was shown to support complete liver-stage development of *P. falciparum* (21). Cell infection rates of the *p52⁻* and *p36⁻* lines were comparable with those of WT *P. falciparum*, indicating that the corresponding protein functions did not support host cell entry. However, the knockouts showed clear defects in liver-stage development. Recently, in an independent study, disruption of the *P52* gene in *P. falciparum* has been achieved by single-cross-over integration (32). The observed phenotype was in agreement with the *p52⁻* phenotype presented here. However, single-cross-over recombination insertions are prone to reversion by plasmid excision, and indeed, the study by van Schaijk et al. (32) observed reverting parasites that had restored WT growth. Our strategy for gene deletions was to use double-cross-over recombination gene replacement, which makes it impossible for the parasite to genet-

ically restore the WT locus, and the parasite is haploid in blood stage, during which the genes are deleted. Additional genes that encode members of the 6-Cys family are encoded in the *Plasmodium* genome, but so far there is no evidence that they could compensate for the function of P52 and P36. Yet, we cannot completely rule out that the attenuated strains might revert in extremely rare instances. It is noteworthy that P52 and P36 are each apparently important for liver infection. Although the genes are paralogues and share a similar expression profile, our results show that neither compensates functionally for the loss of the other. The *P. falciparum p52*$^-$ and *p36*$^-$ phenotypes are therefore similar to the phenotypes observed for the corresponding rodent malaria knockouts (11, 12). Such experimental concurrence of phenotypes between rodent malaria parasite mutants and *P. falciparum* mutants is important because it has been observed that knockout of orthologous genes in rodent and human malaria parasites can result in distinct phenotypes (33, 34).

Single-gene deletions of *P52* and *P36* in rodent parasites led to occasional breakthrough blood-stage infections when high numbers of knockout sporozoites were injected (11, 12). Clearly, breakthrough blood-stage infections in human GAP vaccinations will not be acceptable. In the *P. yoelii* model, a *p52*$^-$/*p36*$^-$ double-knockout GAP did not show any breakthrough infection when inoculated at high doses of 10^5 sporozoites (28). Furthermore, this model of a GAP vaccine induced sterile protection against high-dose i.v. challenge with 10^4 WT sporozoites and against challenge by infectious mosquito bite (28).

We have here produced *P. falciparum p52*$^-$/*p36*$^-$ parasite lines carrying deletions of both *P52* and *P36*. The phenotype of the created double-gene knockout exhibited a more profound intrahepatocytic growth arrest in vitro compared with the single-gene knockout lines. Importantly, intrahepatocytic parasites did not survive beyond the third day of infection and are therefore unable to persist in a growth-arrested state. To further assess the developmental phenotype of the double-knockout parasites in vivo, we tested *p52*$^-$/*p36*$^-$ in an immunodeficient chimeric mouse model that carries human hepatocyte transplants (23, 24). The *p52*$^-$/*p36*$^-$ parasites were able to infect chimeric mouse livers and were clearly detected one day after sporozoite inoculation. However, they were not detected 4 days after infection by either immunohistochemical methods with parasite-specific antibodies or RT-PCR for the 18S ribosomal RNA of *P. falciparum*. In contrast, WT parasites were detected in the chimeric livers 4 days after infection by RT-PCR as well as immunohistochemical methods. The findings in conjunction with the in vitro observations demonstrate that the knockout parasites remain infectious but do not develop and do not persist in the host cells. Previous experience with irradiation-attenuated rodent malaria parasites indicated that persistence of liver stages might be a prerequisite for protection (35). However, more recent data obtained for the *p52*$^-$/*p36*$^-$ GAP rodent malaria line showed clearly that persistence of parasites is not necessary to induce and maintain protection against sporozoite challenge (28).

Together, our results demonstrate the critical role of P52 and P36 in *P. falciparum* hepatocyte infection. The phenotype of arrested liver-stage development exhibited by the *p52*$^-$/*p36*$^-$ *P. falciparum* justifies its testing as a live-attenuated vaccine candidate. Based on the promising preclinical data gathered, the *P. falciparum p52*$^-$/*p36*$^-$ GAP line could be selected for advancing into proof-of-concept (POC) clinical development with administration to human volunteers via bite of *A. stephensi* mosquitoes (36). To support the POC investigational new drug program, it will be critical to produce a *p52*$^-$/*p36*$^-$ GAP Master Cell Bank under phase-appropriate current Good Manufacturing Practice conditions and characterize it per respective Food and Drug Administration and International Conference of Harmonization guidance. Next, it would be important to conduct a phase 1/2a study of the *p52*$^-$/*p36*$^-$ GAP vaccine candidate with administration via mosquito bite to healthy malaria-naive adults. Phase 1 would involve a dose-escalation step to assess safety and tolerability. If safety criteria are met, the phase 2a study would commence with *p52*$^-$/*p36*$^-$ GAP vaccination followed by challenge with *P. falciparum* WT-infected mosquitoes to assess safety, preliminary efficacy, and immunogenicity of the GAP malaria vaccine candidate. With demonstration of protective efficacy, subjects would be rechallenged 6 months later to assess longevity of protection.

Clinical development of a parenteral formulation of genetically attenuated sporozoites is essential. A demonstration that the *p52*$^-$/*p36*$^-$ GAP is safe, well-tolerated, and offers protection against malaria challenge, would allow for further clinical investigation in areas that are endemic for malaria by using a second-generation parenteral GAP vaccine product.

A designed *P. falciparum* live vaccine candidate that has been attenuated by gene deletion as presented here offers the advantages of genetic homogeneity, standardization, batch-to-batch consistency, testable genetic identity, and possibly improved safety of the vaccine with regard to breakthrough infections. These are critical factors on the path to development of a live-attenuated human malaria vaccine.

Materials and Methods

Additional materials and methods are included in the *SI Text*.

Design and Production of Gene-Targeting Constructs. Targeting sequences for *P. falciparum P52* and *P36* were cloned into plasmid pCC1 to facilitate positive–negative selection (18). Restriction sites in the multiple-cloning site (MCS) were SacII/SpeI for the 5′ flank and AvrII/SfoI for the 3′ flank. Sequencing was performed to confirm inserts. Primer sequences can be found in the *SI Text*.

Transfection of *P. falciparum* with Targeting Constructs. Transfection of *P. falciparum* with targeting constructs was preformed as described previously (37, 38). This was followed by negative selection against the cytosine deaminase/uracil phosphoribosyl transferase gene product with 5-fluorocytosine to obtain a parental line with double-cross-over homologous recombination, which results in specific gene deletion. More information about transfection can be found in *SI Text*.

Design and Generation of *p52*$^-$/*p36*$^-$ Double-Gene Deletion Parasite Lines. To produce *p52*$^-$/*p36*$^-$ double-gene knockout parasites, we followed the methods described above for *P52* or *P36* single-gene disruption, except that the NF54 line was used as recipient parasite because the NF54 line is a more stable gametocyte producer then 3D7 under continuous culture. We considered this important because this line might move forward into production as a vaccine candidate. NF54 and 3D7 showed no differences in sporozoite cell invasion and liver-stage development (Tables S8 and S9), and thus direct comparison between knockouts is possible.

RT-PCR and Southern Blotting. A total of 2.4 million *P. falciparum* sporozoites per parasite line were used for RNA extraction with TRIzol (Invitrogen) and were treated with amplification-grade DNAseI (Invitrogen). cDNA was synthesized with SuperScript III Platinum RT-PCR kit (Invitrogen). Amplification with *P52* and *P36* gene-specific primers was done for 35 cycles at 94 °C −30 sec, 55 °C − 30 sec, and 60 °C −2 min. Primers used for P52 were: forward 5′-CCAGAAAATTGCCCTTCTAGAGCCTTTGTT-3′, reverse 5′- GCCCAATACATCATTTGAATAAGCATG-3′; and for *P36* were: forward 5′-TGTTTACACTCGAATGTGGGATGGCATCCT-3′, reverse 5′-GAATGGCATGTAAATTCCCACATTATATCT-3′. Southern blotting methodology is described in detail in *SI Text*.

Mosquito Infections. Gametocyte cultures of WT *P. falciparum* and knockout lines were cultured in vitro by using pooled human A$^+$ sera (Interstate Blood Bank), RPMI-Hepes (Life Technologies/GIBCO), hypoxanthine (Sigma), and washed, type O$^+$ erythrocytes. Media were changed daily, and exflagellation was observed at room temperature by phase-contrast microscopy at 200× magnification beginning 12 to 13 days after the cultures were initiated. Parasites from the cultures were fed to the mosquitoes when the majority of the gametocytes were morphologically mature and vigorous exflagellation was observed. *A. stephensi* aged 4–7 days were prestarved for 2–4 h and then fed for a minimum of 30 min on a 37 °C culture by using a membrane feeder apparatus with bandruche membrane (Joseph Long Inc.). One cage of 250–300 mosquitoes was exposed to concentrated erythrocytes from a 30-mL gametocyte culture mixed with an equal volume of fresh erythrocytes and 2 volumes of serum. Mosquitoes were incu-

bated at 27 °C, 80% humidity, and sporozoites were harvested at 16–22 days after infection.

Sporozoite Counts and Motility Assays. A total of 20,000 sporozoites were seeded per well on 12-well glass slides previously coated with 3% BSA in RPMI-1640. The slides were incubated at 37 °C for 1 h. They were fixed for 10 min with 4% paraformaldehyde at room temperature and washed with 1% FBS in 1× PBS. Slides were blocked with 10% FCS/PBS overnight at 4 °C. Sporozoite trails were immunostained by incubation with anti-PfCSP monoclonal antibody for 45 min at 37 °C and were washed with 1% FCS/PBS. Slides were incubated with anti-mouse IgG AlexaFluor 488 (1:200; Molecular Probes) for 45 min at 37 °C and washed with 1% FCS/PBS. Slides were mounted by using Vectashield mounting medium (Vector Laboratories) and were evaluated at 400× magnification by epifluorescence microscopy (Olympus BX 50 microscope). Quantification was performed by direct microscopic counting of triplicate wells. For *p52*$^{-}$/*p36*$^{-}$ parasite lines, the experiment was performed in 3 independent experiments.

In Vitro Invasion and Development Assays. Invasion assay was preformed as described previously (39). For more details, please refer to *SI Text*. Development assays were performed by adding 60,000 sporozoites per well to HC-04 cell monolayers in 8-well Permanox Labtek chamber slides (Thermo Fisher Scientific). Excess sporozoites were removed, and cells were washed after 3-h incubation at 37 °C and 5% CO_2. Cultures were maintained with daily medium changes for 72, 96, and 144 h. Chamber slides were methanol-fixed and stained by using an mAb against HSP70 (mAb 4C9) (40), CSP (mAb 2A10) (41), LSA-1 (42), and EBA175 (MRA-2; MR4; American Type Culture Collection) as the primary antibody and AlexaFluor 488 anti-mouse IgG (Molecular Probes) as the secondary antibody diluted in 0.1% Evans blue/PBS in a similar manner as described above. Slides were mounted by using Vectashield plus DAPI (Vector Laboratories). The total number of liver stages per well were counted in triplicate wells in 3 independent experiments by using an Olympus BX 50 epifluorescent microscope. Parasites were observed by epifluorescence microscopy at 400× magnification. Photographs were taken by using a BioRad Radiance 2100 Confocal microscope.

In Vivo Assessment of Infection in a Hepatic Chimera Murine Model. To assess defects in the liver-stage development for *p52*$^{-}$, *p36*$^{-}$, and *p52*$^{-}$/*p36*$^{-}$ knockout parasites, we used a human hepatic chimera murine model developed by Mercer et al. (24). Methodology to evaluate *P. falciparum* infection and liver-stage development in the chimera mice was described by Sacci et al. (23). For a more detailed description, please refer to the *SI Text*.

Statistical Analysis. Quantitative differences in salivary gland sporozoites, gliding motility activity, hepatocyte invasion, and liver-stage development between WT and mutant parasite lines were evaluated statistically by using the Wilcoxon matched-pairs signed-rank test at the 95% confidence level with STATA version 10.1 (StataCorp). Paired tests were performed to account for temporal variation in assay conditions.

ACKNOWLEDGMENTS. This work was funded by a grant from the Foundation for the National Institutes of Health through the Grand Challenges in Global Health initiative. Development of the SCID *Alb-uPA* model for *P. falciparum* was funded by National Institutes of Health Grant AI067980 (to J.B.S.).

1. Snow RW, Guerra CA, Noor AM, Myint HY, Hay SI (2005) The global distribution of clinical episodes of Plasmodium falciparum malaria. *Nature* 434:214–217.
2. Nussenzweig RS, Vanderberg J, Most H, Orton C (1967) Protective immunity produced by the injection of x-irradiated sporozoites of plasmodium berghei. *Nature* 216:160–162.
3. Clyde DF, Most H, McCarthy VC, Vanderberg JP (1973) Immunization of man against sporozite-induced falciparum malaria. *Am J Med Sci* 266:169–177.
4. Rieckmann KH, Carson PE, Beaudoin RL, Cassells JS, Sell KW (1974) Letter: Sporozoite induced immunity in man against an Ethiopian strain of Plasmodium falciparum. *Trans R Soc Trop Med Hyg* 68:258–259.
5. Hoffman SL, et al. (2002) Protection of humans against malaria by immunization with radiation-attenuated Plasmodium falciparum sporozoites. *J Infect Dis* 185:1155–1164.
6. Luke TC, Hoffman SL (2003) Rationale and plans for developing a non-replicating, metabolically active, radiation-attenuated Plasmodium falciparum sporozoite vaccine. *J Exp Biol* 206:3803–3808.
7. Mueller AK, et al. (2005) Plasmodium liver stage developmental arrest by depletion of a protein at the parasite-host interface. *Proc Natl Acad Sci USA* 102:3022–3027.
8. Mueller AK, Labaied M, Kappe SH, Matuschewski K (2005) Genetically modified Plasmodium parasites as a protective experimental malaria vaccine. *Nature* 433:164–167.
9. Tarun AS, et al. (2007) Protracted sterile protection with Plasmodium yoelii pre-erythrocytic genetically attenuated parasite malaria vaccines is independent of significant liver-stage persistence and is mediated by CD8+ T cells. *J Infect Dis* 196:608–616.
10. Mikolajczak SA, Jacobs-Lorena V, MacKellar DC, Camargo N, Kappe SH (2007) L-FABP is a critical host factor for successful malaria liver stage development. *Int J Parasitol* 37:483–489.
11. van Dijk MR, et al. (2005) Genetically attenuated, P36p-deficient malarial sporozoites induce protective immunity and apoptosis of infected liver cells. *Proc Natl Acad Sci USA* 102:12194–12199.
12. Ishino T, Chinzei Y, Yuda M (2005) Two proteins with 6-cys motifs are required for malarial parasites to commit to infection of the hepatocyte. *Mol Microbiol* 58:1264–1275.
13. Jobe O, et al. (2007) Genetically attenuated Plasmodium berghei liver stages induce sterile protracted protection that is mediated by major histocompatibility complex Class I-dependent interferon-gamma-producing CD8+ T cells. *J Infect Dis* 196:599–607.
14. Mueller AK, et al. (2007) Genetically attenuated Plasmodium berghei liver stages persist and elicit sterile protection primarily via CD8 T cells. *Am J Pathol* 171:107–115.
15. Kappe SH, et al. (2001) Exploring the transcriptome of the malaria sporozoite stage. *Proc Natl Acad Sci USA* 98:9895–9900.
16. Tsuboi T, et al. (2008) Wheat germ cell-free system-based production of malaria proteins for discovery of novel vaccine candidates. *Infect Immun* 76:1702–1708.
17. Lasonder E, et al. (2008) Proteomic profiling of Plasmodium sporozoite maturation identifies new proteins essential for parasite development and infectivity. *PLoS Pathog* 4:e1000195.
18. Maier AG, Braks JA, Waters AP, Cowman AF (2006) Negative selection using yeast cytosine deaminase/uracil phosphoribosyl transferase in Plasmodium falciparum for targeted gene deletion by double crossover recombination. *Mol Biochem Parasitol* 150:118–121.
19. Fidock DA, Wellems TE (1997) Transformation with human dihydrofolate reductase renders malaria parasites insensitive to WR99210 but does not affect the intrinsic activity of proguanil. *Proc Natl Acad Sci USA* 94:10931–10936.
20. Stewart MJ, Vanderberg JP (1991) Malaria sporozoites release circumsporozoite protein from their apical end and translocate it along their surface. *J Protozool* 38:411–421.
21. Sattabongkot J, et al. (2006) Establishment of a human hepatocyte line that supports in vitro development of the exo-erythrocytic stages of the malaria parasites Plasmodium falciparum and P. vivax. *Am J Trop Med Hyg* 74:708–715.
22. Sim BK, et al. (1990) Primary structure of the 175K Plasmodium falciparum erythrocyte binding antigen and identification of a peptide which elicits antibodies that inhibit malaria merozoite invasion. *J Cell Biol* 111:1877–1884.
23. Sacci JB, Jr., et al. (2006) Plasmodium falciparum infection and exoerythrocytic development in mice with chimeric human livers. *Int J Parasitol* 36:353–360.
24. Mercer DF, et al. (2001) Hepatitis C virus replication in mice with chimeric human livers. *Nat Med* 7:927–933.
25. Greenwood BM, et al. (2008) Malaria: Progress, perils, and prospects for eradication. *J Clin Invest* 118:1266–1276.
26. Alonso PL, et al. (2005) Duration of protection with RTS,S/AS02A malaria vaccine in prevention of Plasmodium falciparum disease in Mozambican children: Single-blind extended follow-up of a randomised controlled trial. *Lancet* 366:2012–2018.
27. Aponte JJ, et al. (2007) Safety of the RTS,S/AS02D candidate malaria vaccine in infants living in a highly endemic area of Mozambique: A double blind randomised controlled phase I/IIb trial. *Lancet* 370:1543–1551.
28. Labaied M, et al. (2007) Plasmodium yoelii sporozoites with simultaneous deletion of P52 and P36 are completely attenuated and confer sterile immunity against infection. *Infect Immun* 75:3758–3768.
29. Corcoran LM, Forsyth KP, Bianco AE, Brown GV, Kemp DJ (1986) Chromosome size polymorphisms in Plasmodium falciparum can involve deletions and are frequent in natural parasite populations. *Cell* 44:87–95.
30. Day KP, et al. (1993) Genes necessary for expression of a virulence determinant and for transmission of Plasmodium falciparum are located on a 0.3-megabase region of chromosome 9. *Proc Natl Acad Sci USA* 90:8292–8296.
31. Goodyer ID, Johnson J, Eisenthal R, Hayes DJ (1994) Purification of mature-stage Plasmodium falciparum by gelatine flotation. *Ann Trop Med Parasitol* 88:209–211.
32. van Schaijk BC, et al. (2008) Gene disruption of Plasmodium falciparum p52 results in attenuation of malaria liver stage development in cultured primary human hepatocytes. *PLoS ONE* 3:e3549.
33. Tewari R, Dorin D, Moon R, Doerig C, Billker O (2005) An atypical mitogen-activated protein kinase controls cytokinesis and flagellar motility during male gamete formation in a malaria parasite. *Mol Microbiol* 58:1253–1263.
34. Dorin-Semblat D, et al. (2007) Functional characterization of both MAP kinases of the human malaria parasite Plasmodium falciparum by reverse genetics. *Mol Microbiol* 65:1170–1180.
35. Scheller LF, Azad AF (1995) Maintenance of protective immunity against malaria by persistent hepatic parasites derived from irradiated sporozoites. *Proc Natl Acad Sci USA* 92:4066–4068.
36. Epstein JE, et al. (2007) Safety and clinical outcome of experimental challenge of human volunteers with Plasmodium falciparum-infected mosquitoes: an update. *J Infect Dis* 196:145–154.
37. Trager W, Jenson JB (1978) Cultivation of malarial parasites. *Nature* 273:621–622.
38. Crabb BS, et al. (2004) Transfection of the human malaria parasite Plasmodium falciparum. *Methods Mol Biol* 270:263–276.
39. Hollingdale MR, Leland P, Leef JL, Schwartz AL (1983) Entry of Plasmodium berghei sporozoites into cultured cells, and their transformation into trophozoites. *Am J Trop Med Hyg* 32:685–690.
40. Tsuji M, Mattei D, Nussenzweig RS, Eichinger D, Zavala F (1994) Demonstration of heat-shock protein 70 in the sporozoite stage of malaria parasites. *Parasitol Res* 80:16–21.
41. Nardin EH, et al. (1982) Circumsporozoite proteins of human malaria parasites Plasmodium falciparum and Plasmodium vivax. *J Exp Med* 156:20–30.
42. Tam JP, Zavala F (1989) Multiple antigen peptide. A novel approach to increase detection sensitivity of synthetic peptides in solid-phase immunoassays. *J Immunol Methods* 124:53–61.

Sterile Protection against *Plasmodium knowlesi* in Rhesus Monkeys from a Malaria Vaccine: Comparison of Heterologous Prime Boost Strategies

George Jiang[1,2], Meng Shi[1], Solomon Conteh[1], Nancy Richie[1], Glenna Banania[1], Harini Geneshan[1], Anais Valencia[1], Priti Singh[1], Joao Aguiar[1], Keith Limbach[1], Kurt I. Kamrud[3], Jonathan Rayner[3], Jonathan Smith[3], Joseph T. Bruder[4], C. Richter King[4], Takafumi Tsuboi[5], Satoru Takeo[5], Yaeta Endo[5], Denise L. Doolan[6], Thomas L. Richie[1], Walter R. Weiss[1,2,5]*

1 Naval Medical Research Center, Malaria Program, Silver Spring, Maryland, United States of America, **2** Henry M. Jackson Foundation, Rockville, Maryland, United States of America, **3** AlphaVax, Research Triangle Park, North Carolina, United States of America, **4** GenVec, Gaithersburg, Maryland, United States of America, **5** Cell-free Science and Technology Research Center, Ehime University, Matsuyama, Ehime, Japan, **6** Queensland Institute of Medical Research, Brisbane, Australia

Abstract

Using newer vaccine platforms which have been effective against malaria in rodent models, we tested five immunization regimens against *Plasmodium knowlesi* in rhesus monkeys. All vaccines included the same four P. knowlesi antigens: the pre-erythrocytic antigens CSP, SSP2, and erythrocytic antigens AMA1, MSP1. We used four vaccine platforms for prime or boost vaccinations: plasmids (DNA), alphavirus replicons (VRP), attenuated adenovirus serotype 5 (Ad), or attenuated poxvirus (Pox). These four platforms combined to produce five different prime/boost vaccine regimens: Pox alone, VRP/Pox, VRP/Ad, Ad/Pox, and DNA/Pox. Five rhesus monkeys were immunized with each regimen, and five Control monkeys received a mock vaccination. The time to complete vaccinations was 420 days. All monkeys were challenged twice with 100 P. knowlesi sporozoites given IV. The first challenge was given 12 days after the last vaccination, and the monkeys receiving the DNA/Pox vaccine were the best protected, with 3/5 monkeys sterilely protected and 1/5 monkeys that self-cured its parasitemia. There was no protection in monkeys that received Pox malaria vaccine alone without previous priming. The second sporozoite challenge was given 4 months after the first. All 4 monkeys that were protected in the first challenge developed malaria in the second challenge. DNA, VRP and Ad5 vaccines all primed monkeys for strong immune responses after the Pox boost. We discuss the high level but short duration of protection in this experiment and the possible benefits of the long interval between prime and boost.

Citation: Jiang G, Shi M, Conteh S, Richie N, Banania G, et al. (2009) Sterile Protection against *Plasmodium knowlesi* in Rhesus Monkeys from a Malaria Vaccine: Comparison of Heterologous Prime Boost Strategies. PLoS ONE 4(8): e6559. doi:10.1371/journal.pone.0006559

Editor: Wasif N. Khan, University of Miami, United States of America

Received July 21, 2008; **Accepted** June 6, 2009; **Published** August 10, 2009

Funding: This work was supported by funds allocated to the Naval Medical Research Center by the US Army Medical Research Material Command (work unit 6000.RAD1.F.A0309). The funders had no role in study design, data collection and analysis, decision to publish, or preparation of the manuscript.

Competing Interests: The authors have declared that no competing interests exist.

* E-mail: walter.weiss@verizon.net

Introduction

Malaria infects over 200 million people annually and causes almost 1 million deaths [1]. An effective vaccine against malaria would be a valuable public health tool, complementing anti-malaria drugs, vector control and environmental modification. Despite intensive research no malaria vaccine is commercially yet available. The vaccine farthest along in field testing [2]is based on a single malaria antigen, and is not as effective as experimental radiation attenuated whole parasite vaccines [3–8]. When immune responses to the protective irradiated parasite vaccines are analyzed, no single target antigen has been identified that explains the full extent of host immunity[9]. This suggests that the protective vaccines work by the summation of many immune responses against multiple antigens on the parasites[9].

Our approach to vaccine development is to develop a multi-antigen malaria vaccine, mimicking the radiation attenuated whole parasite vaccines. However, until recently there has been no animal model allowing the efficacy testing of vaccines against the pre-erythrocytic stages of the human malaria parasite *P. falciparum*. One group in South America has shown that an Owl monkey can be reproducibly infected with sporozoites of *P. falciparum* [10–12]. However access to these protected primates is restricted making this model difficult to replicate elsewhere. While murine malaria models are invaluable for basic laboratory testing, they may not accurately predict human vaccine immunogenicity or efficacy. Furthermore there are no reliable immune correlates of protection for malaria vaccines, so immunogenicity studies without the results of malaria challenge are potentially misleading. Attempting to avoid these difficulties, we have chosen to test malaria vaccine strategies in the *P. knowlesi*/rhesus monkey system.

P. knowlesi is a natural infection of *Macaca fasicularis* (cynomolgus) monkeys[13], but also infects humans in South East Asia[14,15]. P. knowlesi sporozoites are highly infectious for many primates including *M. mulatta* (rhesus) monkeys with 100 P. knowlesi sporozoites given iv reliably infecting rhesus monkeys in our facility. After the P. knowlesi sporozoite invades the hepatocyte, merozoites are released into the bloodstream 4–5

days later, comparable to the 5–6 day hepatic development of P. falciparum in humans. P. knowlesi takes only 24 hours to complete its growth cycle in the red blood cell, as compared to 48 hours for P. falciparum, and exponential growth of P. knowlesi often leads to parasitemias over 50% that can be fatal in rhesus. If the initial surge of parasites does not kill the host, P. knowlesi becomes a chronic low-grade infection with reproducible spikes in parasitemia due to antigenic variation[13,16], similar to chronic P. falciparum infection in humans. P. knowlesi infection can be cured with chloroquine, and monkeys can be successfully re-infected with P. knowlesi sporozoites 4–6 times before significant blood stage immunity is evident ([13] and Weiss, unpublished data), which allows for repeat sporozoite challenges to assess the duration of vaccine protection.

Our goal in designing this experiment was to find a more potent malaria vaccine than the DNA/poxvirus heterologous combination which we have tested previously [17–19]. The vaccines we use combine four malaria antigens: the circumsporozoite protein (CSP), sporozoite surface protein 2 also called thrombospondin-related adhesion protein (SSP2 or TRAP), apical merozoite antigen-1 (AMA1) and merozoite surface protein 1 (MSP1). We refer to this four antigen combination as Pk4. Previously the best protection we have seen in rhesus monkeys was from a Pk 4 'prime-boost' vaccine using DNA plasmids followed by recombinant poxvirus. In this experiment, 2/11 (18%) animals were sterilely protected, with an additional 7/11(63%) showing blood stage protection [18]. However, our studies of this vaccine have highlighted several limitations. First, there was little immune response detectable in the peripheral blood after the DNA vaccinations, which made us wonder if better priming before viral boost would be more efficacious. Secondly, protection by the vaccine waned quickly, and there was little efficacy to a second malaria sporozoite challenge given three months after the first challenge. Also, we did not have the reagents to measure immune responses to all four antigens in the Pk4 vaccine.

The present study uses the Pk4 antigens to compare priming with three different vaccine modalities before poxvirus (Pox) boost: DNA plasmids, recombinant adenovirus 5 (Ad5) [20,21], and recombinant alphavirus-derived viral replicon particles (VRPs) [20,21]. The DNA plasmids and poxviruses constructs used in this study are the same as used in our previous published work [17]. Our group has tested both VRP and Ad5 malaria vaccines in mice, and has found them to be as good as or better than DNA vaccines for priming before a poxvirus boost ([22] and Doolan unpublished data). Our goal was to evaluate these vaccine technologies in a primate malaria model where vaccine responses, host-parasite interactions and protective efficacy may be better predictors of results in humans than can be achieved with rodent malaria models. We also developed reagents to test immune responses to all 4 P. knowlesi vaccine antigens in order to study their association with protection.

Materials and Methods

Animals

Rhesus monkeys (*Macaca mulatta*) descended from Chinese stock were used for this experiment. Animals were obtained by and housed at the Walter Reed Army Institute of Research/Naval Medical Research Center (WRAIR/NMRC), Silver Spring, MD. Animals were selected to be in general good health, and to have no history of prior exposure to malaria. Prior to selection for the studies, serum specimens from all animals were tested in IFAT assays against P. knowlesi sporozoites and P. knowlesi infected red cells, and all animals with positive serum titers at dilutions of 1:80 or higher were excluded. The experiment was conducted according to *Guide for the Care and Use of Laboratory Animals* 1996. The experiment required 6 groups of 5 monkeys each (see Table 1). The 30 selected monkeys were first stratified by age, sex, and weight and then randomly assigned to groups. This resulted in the 6 groups being closely matched, with mean age 6.4 years (SD 0.2) and mean weight 5.2 kg (SD 0.2). There were 2 females and 3 males in each group.

Ethics Statement

Animal use in this study was approved by the WRAIR/NMRC Institutional Animal Care and Use Committee. The WRAIR/NMRC animal facility is AAALAC accredited and animals are housed and cared for according to its guidelines. In this study the major risk to the animals was from the malaria infection. Harm from malaria infection was minimized by treating with antimalarial drugs at a parasitemia level low enough to prevent serious illness.

DNA plasmid vaccines

The DNA plasmid vaccines encoding Pk4 genes have been previously described [17]. Briefly, DNA sequences encoding the full-length genes from the P. knowlesi H strain of CSP, SSP2, and AMA-1 and the 42 kD C terminal fragment of MSP-1 were cloned into the VR1020 mammalian expression vector (Vical Inc, San Diego CA). This vector contains a CMV promoter, and a TPA signal sequence. Each gene was cloned into a separate plasmid. Recombinant DNA plasmids were produced by Vical, Inc and contained less that 0.6 EU of endotoxin per mg and were at least 80% super coiled. Plasmids were diluted in PBS pH 7.2 prior to injection.

Viral vectors

The same sequences of the Pk4 genes were cloned into 3 different viral vectors: VRP, Ad5, and Pox. Each P. knowlesi antigen was cloned into separate virus vector.

The Pox vaccines encoding P. knowlesi genes have been previously described [17,18]. Briefly, the same four P. knowlesi DNA sequences, which were used to construct the P. knowlesi DNA plasmids, were cloned into the COPAK poxvirus immuni-

Table 1. Immunization regimens.

Group[a]	Vaccinations[b]					
	wk 0	wk 4	wk 16	wk 55	wk 60	wk 62
Control	-	-	-	-	pPox[f]	challenge[h]
Pox	-	-	-	-	Pox[g]	challenge
VRP/Pox	VRP[c]	VRP	VRP	-	Pox	challenge
VRP/Ad	VRP	VRP	VRP	-	Ad5	challenge
Ad/Pox	-	-	-	Ad5[d]	Pox	challenge
DNA/Pox	Plasmid[e]	Plasmid	Plasmid	-	Pox	challenge

[a]Rhesus monkeys 5 animals per group.
[b]Vaccines are mixtures of vectors expressing the individual antigens PkCSP, PkAMA1, PkSSP2, and PkMSP1.
[c]Recombinant VRP, 5×10^7 IU/dose each antigen.
[d]Recombinant Ad5 vectors, 2.5×10^{10} particles each antigen.
[e]Recombinant plasmid vaccine 1 mg/dose each antigen.
[f]Parental pox virus without antigen inserts, 8×10^8 pfu total.
[g]Recombinant pox virus, 2×10^8 pfu/dose each antigen.
[h]Challenge with 100 Pk sporozoites iv 12 days after last vaccination.
doi:10.1371/journal.pone.0006559.t001

zation vector (Virogenetics, Troy, N.Y). COPAK is derived from the Copenhagen strain of vaccinia virus. The recombinant alphavirus derived VRP particles for the Pk4 vaccine were constructed and produced by AlphaVax, Inc (Research Triangle Park, NC), and the recombinant attenuated Ad 5 for the Pk4 antigens were produced by the GenVec, Inc (Gaithersburg, MD).

Immunization regimens

Five Pk4 malaria vaccine regimens were compared to a mock control vaccine in this experiment (Table 1). At the time of each injection, the four antigen vaccines (either DNA or viruses) were mixed and then given im in the right quadriceps muscle in a total volume of 1 ml. DNA injections were given by a needle-free injection system Biojector 2000 (Bioject, Inc, Tualatin, OR), while all other injections were with #20 gauge needle and syringe. As seen in Table 1, groups received either no priming injections, or were primed with DNA plasmids, VRPs, or Ad5. DNA priming injections contained 1 mg of each of the four Pk4 plasmids, and were given at weeks 0, 4, and 16. VRP priming injections contained 5×10^7 infectious units (IU) encoding each Pk4 antigen, and were also given at weeks 0, 4, and 16. The Ad5 priming injection contained 2.5×10^{10} particles encoding each Pk4 antigen and was given at week 55.

All monkeys were boosted at week 60. The Control group was given 8×10^8 pfu of parental COPAK virus lacking a transgene insert. The four groups receiving Pox vaccine were given a mix of 2×10^8 pfu of each of four COPAK viruses encoding one of the four Pk4 antigens. The one group boosted with Ad5 received a mix of 2.5×10^{10} particles of each of the four Ad5 viruses encoding one of the four Pk4 antigens (same dose as the Ad5 prime).

Malaria sporozoite challenges and parasitemia measurement

The first P. knowlesi sporozoite challenge was given on day 12 after viral boost (week 62). Our initial plan was to challenge 2–4 weeks after viral boost as we had done in our previous studies [17–19]. However, the challenge was done two days early when it appeared that this was the best date to obtain infectious sporozoites from our mosquitoes. P. knowlesi H strain sporozoites were grown in *Anopheles dirus* mosquitoes. Sporozoites were harvested 14 days after mosquitoes had fed on an infected rhesus monkey. Harvesting was by the Ozaki method. Sporozoites were diluted in E199 medium with 5% normal rhesus serum and counted with a hemocytometer. 100 sporozoites in a total volume of 1 ml were injected IV. A random challenge order was used for monkeys from different groups, with the exception that the first and last monkeys challenged were from the Control group. The challenge took place over the course of four hours.

Beginning 6 days after sporozoite challenge, each day at 1 PM blood was taken by ear prick. P. knowlesi infections are highly synchronized in the blood. Before noon parasites are schizonts, up to half of which may adhere to blood vessels making counts of circulating parasites inaccurate. With low levels of parasitemia, most schizonts rupture around mid-day to produce a new crop of ring forms. Taking blood samples at 1pm avoids underestimating parasite load during the early days of infection. At higher parasitemia levels, schizont rupture is often delayed several hours. If many schizonts are present in the 1 PM specimen, blood smears were repeated later in the day to get accurate parasite counts. Blood was prepared for thin and thick malaria smears using Giemsa stain at pH 7.01 using standard methods [23] For thin smears, 20,000 red cells were examined. For thick smears, 0.025 μl of blood was examined. These data was used to calculate the percent infected red blood cells. Animals were followed for 40 days after challenge. To prevent death of animals, when parasitemias exceeded 2% monkeys were treated by IM injection of chloroquine hydrochloride 20 mg/kg on day 1 and 10 mg/kg on days 3 and 4. Forty days after the first sporozoite challenge all previously untreated monkeys received chloroquine to eliminate any possible undetected malaria infections prior to rechallenge.

The second P. knowlesi sporozoite challenge was given four months after the first sporozoite challenge using the same procedures for infection and follow-up of parasitemias.

Blinding for antibody and T cell assays. Operators conducting the antibody and T cell assays were not aware of the vaccination group or the parasitemia status of animals when they performed the assays. When T cell assays had to be run in batches, a study investigator who was not involved in the in vitro testing selected the samples, such that animals from all groups were included in every run to exclude inter-group bias.

Antibody ELISA assay

Plasma sample was tested by ELISA for IgG titer using each of the four P. knowlesi antigens used in the immunization studies as capture antigens. Capture antigen for P. knowlesi CSP was a synthetic peptide of 36 amino acids representing 3 copies of the 12 aa repeat motif GDGANAGQPQAQ. Capture antigen for the other three proteins consisted of full length P. knowlesi SSP2, full length P. knowlesi AMA-1 ectodomain and the P. knowlesi MSP-1 42 kD fragment, respectively, each produced by in vitro synthesis using the Rapid Translation System RTS 500 E. coli HY kit (Roche Diagnostics Corporation, Indianapolis, IN). These capture antigens were used at concentrations of 1 to 4 micrograms per ml in PBS pH 7.2 in Immulon II 96 well plates (Dynex Technologies Inc., Chantilly, VA). Plates were blocked with 5% milk powder in PBS for 2 hours. Plasma samples were diluted in 3% non-fat dry milk in PBS and incubated in plates at room temperature for 4–18 hours. Peroxidase-labeled goat anti-human IgG (H+L) (Kierkegard Perry Laboratories, Gaithersburg MD) at a 1:10,000 dilution in 3% non-fat dry milk was added for 1 hour, and subtrate was ABTS (Kierkegard Perry Laboratories). OD was read using a SPECTRA MAX 190 ELISA reader (Molecular Devices Corp., Sunnyvale, CA). Endpoint titer for each sample was the highest plasma dilution at which the OD was equal or greater than 3-fold the value of plasma from naïve monkeys.

Immunofluroescence Antibody titers (IFAT) against whole parasite preparations

For each animal, plasma from five days before the first sporozoite challenge was evaluated in IFAT against both P. knowlesi air dried sporozoites and P. knowlesi infected red blood cells as previously described [24]. Results were the last dilution of plasma at which fluorescence could be seen.

Antigens for in vitro studies of T cells

For in vitro T cell studies of the four P. knowlesi strain antigens, we restimulated cells using synthetic peptides for the CSP and AMA1 antigens, and recombinant proteins for the SSP2 and MSP1 antigens. For all studies, negative control wells were run with medium alone, and positive control wells were run with concanavalin A. Synthetic peptides for the CSP and AMA1 antigens were produced by Pepscan (Lelystad, The Netherlands). Each peptide was 15 amino acids long with 10 amino acids overlapping the adjacent peptide, and the peptide series covered the entire length of each P. knowlesi protein. The CSP pool contained 42 peptides and the AMA1 pool contained 104 peptides. The final concentration of each individual peptide in

the pool was 2.5 μg/ml for the CSP and 1.2 μg/ml AMA1. These concentrations were selected based on our previous studies, and testing with samples from a small number of positive and negative control samples.

The recombinant P. knowlesi SSP2 and MSP1 (42 kD) proteins used for in vitro T cell restimulation were generated using an in vitro wheat-germ cell free expression system. This protein expression method has been described in detail[25–27]. Briefly, transcription of mRNA was achieved using SP6 RNA polymerase (Promega, Madison, WI). The reaction mixture resulting from transcription is then directly used as mRNA source in the translation step. Proteins were translated using a cell-free bilayer system [26], where the translation reaction is separated from translational substrate buffer by carefully overlaying in a 6-well multi-well plate. Then the plate was incubated at 26°C for overnight. Proteins from the reaction were bound to a glutathione sepharose 4B column (GE Healthcare Bio-Sciences, Piscataway, NJ), washed with PBS, and then the column was treated with TEV protease (Invitrogen, 60 U/column) at 30°C for 3 hrs. Proteins were eluted with PBS and fractions were analyzed by 12.5% SDS-polyacrylamide gel stained with CBB. Aliquots were stored at −80°C and proteins were used at a final concentration of 5 μg/ml in in vitro T cell studies.

IFN-γ ELISPOT assay

For in vitro T cell studies, PBMC were isolated from peripheral blood by centrifugation over ficoll and preserved in liquid nitrogen. Cells from all time points for each animal were run on the same day to facilitate comparisons.

The assay for rhesus IFN-γ was modified from our previous method [28,29]. In brief, PVDF-96 well plates (Millipore Corporation, Bedford, MA) were coated with anti-human IFN-γ (clone GZ-4, Bender Med Systems, Burlingame, CA) incubated overnight at 4°C, blocked and washed. Cryopreserved PBMC were rested overnight after thawing, and 2×10^5 cells added per well. Quadruplicate cells were restimulated with one of the four P. knowlesi H strain antigens (as described above), or controls. ELISPOT plates were incubated for 18 hrs at 37°C in an atmosphere of 5% CO_2. The IFN-γ spot-forming cells (SFCs) were counted using an AID ELISPOT reader (Cell Technology, Inc, Columbia, MD, USA). Responses are presented as the mean number of net SFCs per million cells in stimulated wells minus the mean number of spots in medium controls. The major differences from our previous methods are the resting of the PBMC after thawing, the use of PVDF instead of MAIP plates, and counting of spots with the AID ELISPOT reader.

Intracellular cytokine staining and flow cytometric studies

All reagents for the intracellular cytokine staining were purchased from BD Bioscience (San Jose, CA) unless otherwise mentioned. A total $0.5\text{-}1\times10^6$ cryopreserved PBMC were plated per well in U-bottomed 96-well plates, with 1 μg/ml anti-human CD28 (Clone CD28.2) and 1 μg/ml anti-human CD49d (Clone 9F10) antibodies with or without antigen. Malaria antigens and positive and negative control antigens were the same as for the ELISPOT studies. Brefeldin A was added at 10 μg/ml at 2 hrs after initial incubation, and plates then incubated an additional 14-hrs at 37°C in an atmosphere of 5% CO_2. The cells were stained with one or more of the following antibodies: CD3-PE-Cy7, CD4-Alex430, and CD8-APC-Cy7. After the surface staining, cells were permeabilized in 100 μl CytoFix/Cytoperm buffer for 20 min, and then stained with anti- IFN-γ- FITC (Clone B27), and anti-IL2-APC(Clone MQ1-17H12), for 45 min on ice in the dark. The stained samples were analyzed using the LSR-II flow cytometer (Becton Dickinson Immunocytometry Systems, San Jose, CA). The expression level of intracellular cytokines was presented as the percentage of stained cells in gated cell populations minus background responses in the absence of antigen. The non-specific background was generally between 0.001–0.05%.

Statistical analyses

Parasitemia outcomes were analyzed using Kaplan-Meier survival curves and the Log rank test has been used to compare survival curve for two or more groups. Immunogenicity of vaccine groups was analyzed using ANOVA and Tukey's Adjusted Significant Difference Test. We used the Cox Proportional Hazard model to analyze effects of immune responses on protection against malaria.

Results

Effect of vaccinations on parasitemias

Figure 1 shows the parasitemia curves for all monkeys after the first sporozoite challenge. Each of the panels shows animals that received a different vaccine. In the Control group (Figure 1A), the first blood stage parasites were detected between days 8 to 10 (mean 8.6 days) and animals required drug treatment for parasitemia exceeding 2% between days 10 to 12 (mean 10.8 days). This is consistent with our previous studies using the 100 P. knowlesi sporozoite challenge in rhesus monkeys [17–19]. Animals receiving only recombinant Pk4 Pox vaccine 12 days before challenge (Figure 1B) had parasitemias similar to the Control group, with no protection against sporozoite or blood stage parasites.

Compared with the Control groups, monkeys receiving the VRP/Pox regimen (Figure 1C) had a 2.4 day delay to first parasitemia (mean 11 days) and a 3.2 day delay to parasitemia>2% (mean 14 days). Similar delays to the first parasites being detected were seen in the VRP/Ad group (Figure 1D), with monkey #252 having an unusual pattern of infection. This animal did not have detectable parasites in thick or thin malaria blood films until days 15–19, when single parasites were observed intermittently. Then, starting on day 20, parasitemia rose steadily for one week, peaking at 1%, followed by a decline that occurred in the absence of drug treatment. We suspect this animal was parasitemic at a level below detection prior to day 15, and then had a increase in parasites due to antigenic variation [30], a pattern of recrudescence well known in P. knowlesi infections and one we have observed previously in our own studies [17,18]. The control of parasitemia below lethal levels without need of drugs we term 'self-cure,' although it is likely that blood stage parasites remain at very low levels after they fall below the threshold detectable by microscopy.

Figure 1E shows results from the Ad/Pox vaccine group. For three of the animals in this group there was a modest 0.9 day delay in day to first parasitemia (mean 9.5 days) and 1.5 day delay in the day>2% level (mean 12.3 days), relative to Controls. A fourth animal reached 1% parasitemia and then self-cured. The fifth animal never developed detectable parasitemia during the 40 days of follow up. We think that this animal was sterilely protected by the Ad/Pox vaccine and never had P. knowlesi parasites exit the liver and infect red blood cells, because there were no later spikes of recrudescent parasitemia (as observed in the self-cure monkey #252 from Panel D) during the 40 days of follow-up.

Figure 1F shows the parasitemias of the DNA/Pox vaccine group. Three of five monkeys were sterilely protected, with 2 monkeys showing a 0.9 day delay in first day of parasitemia (mean